

ISTANBUL OKAN UNIVERSITY  
INSTITUTE OF SCIENCES AND ENGINEERING



DEVELOPING DE-NOISING ALGORITHM IMPROVED WITH LEAST MEAN  
SQUARES FILTER FOR AUTONOMOUS-VEHICLES LIDAR IN SNOWFALL

A THESIS

submitted by

CEMRE KAVVASOGLU

in partial fulfillment of the requirements for the degree of

MASTER OF SCIENCE

AUGUST 2019

Program: Power Electronics and Clean Energy Systems

ISTANBUL OKAN UNIVERSITY  
INSTITUTE OF SCIENCES AND ENGINEERING  
DEPARTMENT OF ELECTRICAL AND ELECTRONICS ENGINEERING

DEVELOPING DE-NOISING ALGORITHM IMPROVED WITH LEAST MEAN  
SQUARES FILTER FOR AUTONOMOUS-VEHICLES LIDAR IN SNOWFALL

MASTER OF SCIENCE

THESIS

CEMRE KAVVASOGLU

SUPERVISOR: ASST. PROF. DR. OMER CIHAN KIVANC

AUGUST 2019

PROGRAM: POWER ELECTRONICS AND CLEAN ENERGY SYSTEMS

DEVELOPING DE-NOISING ALGORITHM IMPROVED WITH LEAST MEAN  
SQUARES FILTER FOR AUTONOMOUS-VEHICLES LIDAR IN SNOWFALL

A THESIS

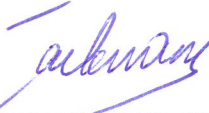
by


CEMRE KAVVASOGLU


submitted to the Institute of Sciences and Engineering of  
ISTANBUL OKAN UNIVERSITY

in partial fulfillment of the requirements for the degree of  
MASTER OF SCIENCE

Approved by:

  
Asst. Prof. Dr. Omer Cihan  
Kivanc  
Supervisor

  
Prof. Dr. Ramazan Nejat  
Tuncay  
Member

  
Asst. Prof. Dr. Duygu  
Bayram Kara  
Istanbul Technical University  
Member

AUGUST 2019

Program: Power Electronics and Clean Energy Systems

## ABSTRACT

### DEVELOPING DE-NOISING ALGORITHM IMPROVED WITH LEAST MEAN SQUARES FILTER FOR AUTONOMOUS-VEHICLES LIDAR IN SNOWFALL

The environmental perception is major requirement for autonomous vehicles. While the detection of the environment in autonomous vehicles is provided by LIDAR, camera and radar, some adverse environmental conditions deteriorate this detection process. Particularly when driving in heavy snow, the snowflakes reduce the vision quality by preventing the images of the objects behind them. In this study, for the LIDAR sensor the De-noising Algorithm is used which is improved by Least Mean Squares (LMS) Filter in order to purify the LIDAR data in snowy weathers. Furthermore, the positions of the objects behind the snowflakes, which are not shown, are estimated by referring the data recorded earlier. In order to develop this algorithm, the LIDAR sensor data in snowy weather is recorded via the Nvidia Jetson TX1 developer platform and the Robot Operating System (ROS). An algorithm is developed to detect sudden distance changes due to snowflakes in sensor data using a variable threshold value. The proposed algorithm is performed by real-time tests on an autonomous vehicle using an artificial snow machine. The existing median filter results are compared with the results of the developed algorithm. The experimental results show that the proposed algorithm presents 99% de-noising success even under heavy snowfalls.

**Keywords:** De-noising, Least Mean Squares Filter, Adverse Weather Conditions, LIDAR, Autonomous Vehicles

## KISA ÖZET

### OTONOM ARAÇLAR'DA LIDAR İÇİN KAR YAĞIŞINDA EN KÜÇÜK ORTALAMALI KARELER FİLTRESİYLE GÜÇLENDİRİLMİŞ GÜRÜLTÜ GİDERİCİ ALGORİTMA GELİŞTİRİLMESİ

Otonom araçlar için çevresel algı ana gereksinimdir. Otonom araçlarda çevrenin tespiti LIDAR, kamera ve radar tarafından sağlanırken, bazı olumsuz çevresel koşullar bu tespit sürecini kötüleştirir. Özellikle şiddetli kar yağışı sırasında kar taneleri, arkalarındaki nesnelere görüntülerini engelleyerek görüş kalitesini düşürür. Bu çalışmada LIDAR sensörü için, LIDAR verilerini karlı havalarda arındırmak amacıyla En Küçük Ortalamalı Kareler Filtresi ile güçlendirilen gürültü giderici algoritma geliştirilmiştir. Ayrıca, kar taneleri arkasındaki gösterilmeyen nesnelere pozisyonları daha önce kaydedilen verilere bakılarak tahmin edilmektedir. Bu algoritmayı geliştirmek için, karlı havalarda LIDAR sensör verileri Nvidia Jetson TX1 geliştirici platformu ve Robot İşletim Sistemi (ROS) ile kaydedilmektedir. Sensör verilerindeki kar tanelerinin neden olduğu ani mesafe değişikliklerini tespit etmek için değişken bir eşik değeri kullanılarak algoritma geliştirilmiştir. Önerilen algoritma yapay bir kar makinesi kullanılarak otonom bir araç üzerinde gerçek zamanlı testlerle denenmiştir. Mevcutta bulunan median filtre sonuçlarıyla geliştirilen algoritmanın sonuçları kıyaslanmıştır. Deneysel sonuçlar, önerilen algoritmanın yoğun kar yağışı altında bile %99 gürültü azaltma başarısı gösterdiğini göstermektedir.

Anahtar Kelimeler: Gürültü Giderici, En Küçük Ortalamalı Kareler Filtresi, Olumsuz Hava Koşulları, LIDAR, Otonom Araçlar



To My Family

## ACKNOWLEDGMENTS

Firstly, I would like to express my special gratitude and thanks to my adviser, Asst. Prof. Dr. Ömer Cihan Kıvanç for imparting his knowledge and expertise in this study. He always provided me full support since my undergraduate studies. He never lost faith in me and supported me under all circumstances. I am grateful to him for expanding my horizon, for all his knowledge and experiences he has given me not only academically, in all areas throughout seven years with my undergraduate and graduate education.

Right after, I would like to thank Prof. Dr. Ramazan Nejat Tuncay. He moved me forward during my graduate studies and my assistantship at his undergraduate level courses. He always tried to teach me something and always trusted me. He is a wonderful person who, despite his decades of experience, has always maintained his modesty. I feel very lucky to be his student and assistant.

I am highly indebted to Prof. Dr. Semih Bilgen, Asst. Prof. Dr. Salih Barış Öztürk, Asst. Prof. Dr. Didem Kıvanç Türeli, Tahir Eren Mungan, Berkin Atila, Zeynel Koç for their guidance and continuous help.

I would like to thank the Faculty of Engineering Members at Istanbul Okan University for their guidance and motivation during my study.

My sincere gratitude goes to my family for their continuous support and patience during my life.

Finally, I would like to thank Istanbul Okan University UTAS Center for allowing us to use Autonomous Research Vehicle "OKANOM".

## TABLE OF CONTENTS

LIST OF TABLES . . . . .	vii
LIST OF FIGURES . . . . .	viii
SYMBOLS . . . . .	x
ACRONYMS . . . . .	xi
1. INTRODUCTION . . . . .	1
1.1. Literature Review . . . . .	3
1.2. Hypothesis . . . . .	8
1.3. Outline of Thesis . . . . .	9
2. DE-NOISING ALGORITHM DEVELOPMENT & METHODOLOGY	10
2.1. Tools . . . . .	10
2.1.1. Laser Imaging Detection and Ranging . . . . .	10
2.1.2. NVIDIA - Jetson TX1 Developer Kit . . . . .	12
2.1.3. Robot Operating System . . . . .	13
2.2. Proposed De-Noising Algorithm Approach . . . . .	13
2.2.1. Median Filter . . . . .	13
2.2.2. Least Mean Squares Filter . . . . .	14
2.2.3. Proposed Method . . . . .	15
3. EXPERIMENTAL RESULTS . . . . .	19
4. CONCLUSION . . . . .	36
4.1. Future Work . . . . .	36
REFERENCES . . . . .	38
VITA . . . . .	46



## LIST OF TABLES

TABLE	Page
2.1. Features of LMS111-10100 . . . . .	11
2.2. Performance of LMS111-10100 . . . . .	11
2.3. Technical Specifications of Nvidia Jetson TX1 Developer Kit . . . . .	13
3.1. Compare of Filters - Real Snow . . . . .	23
3.2. Compare of Filters - Artificial Snow 1 . . . . .	28
3.3. Compare of Filters - Artificial Snow 2 . . . . .	33
3.4. Compare of Filters - All Artificial Snow Tests . . . . .	34

## LIST OF FIGURES

FIGURE	Page
2.1. Connection of Tools . . . . .	10
2.2. LIDAR (SICK, LMS111-10100) . . . . .	11
2.3. Working Range Diagram of LMS111-10100 . . . . .	12
2.4. Nvidia Jetson TX1 Developer Kit . . . . .	13
2.5. Sunday, 24 February 2019 - Snowfall . . . . .	15
2.6. Noise Detection Flowchart . . . . .	17
2.7. Pseudocode of Proposed Method . . . . .	18
2.8. Flowchart of De-Noising Algorithm Improved with Least Mean Squares Filter . . . . .	18
3.1. Autonomous Research Vehicle, OKANOM . . . . .	19
3.2. Artificial Snowfall . . . . .	20
3.3. First Frame of Snowy Weather . . . . .	21
3.4. The Highest Noisy Frame of Snowy Weather . . . . .	21
3.5. Marked Noisy Frame of Snowy Weather . . . . .	22
3.6. Original Data, (4763. Frame) - 8 Noisy Points . . . . .	24
3.7. Median (5) Filter, (4763. Frame) - 2 Noisy Points . . . . .	25
3.8. Median (15) Filter, (4763. Frame) - No Noisy Points . . . . .	25
3.9. De-noising Filter, (4763. Frame) - No Noisy Points . . . . .	26
3.10. De-noising with Median Filter, (4763. Frame) - No Noisy Points . . . . .	26
3.11. De-noising with LMS Filter, (4763. Frame) - No Noisy Points . . . . .	27
3.12. Noise Numbers of Frames (Real Snow) . . . . .	27
3.13. Original Data, (1634. Frame) - 34 Noisy Points . . . . .	29

3.14.	Median (5) Filter, (1634. Frame) - 24 Noisy Points . . . . .	29
3.15.	Median (15) Filter, (1634. Frame) - 16 Noisy Points . . . . .	30
3.16.	De-noising Filter, (1634. Frame) - No Noisy Points . . . . .	30
3.17.	De-noising with Median Filter, (1634. Frame) - No Noisy Points . . . . .	31
3.18.	De-noising with LMS Filter, (1634. Frame) - No Noisy Points . . . . .	32
3.19.	Noise Numbers of Each Frame at First Artificial Snow Record . . . . .	32
3.20.	Noise Numbers of Each Frame at Second Artificial Snow Record . . . . .	33
3.21.	Comparison of Filter Success Rates due to Snow Density . . . . .	34

## SYMBOLS

$\lambda$  Lambda

$\mu$  Mu



## ACRONYMS

**LIDAR** Laser Imaging Detection and Ranging

**LMS** Least Mean Squares

**SNR** Signal to Noise Ratio

**ROR** Radius Outlier Removal

**DROR** Dynamic Radius Outlier Removal

**PCA** Principal Component Analysis

**UWB** Ultra-Wideband

**V2V** Vehicle to Vehicle

**V2I** Vehicle to Infrastructure

**ABS** Anti-Lock Braking System

**ADMF** Adaptive Mean Filter

**HOS** Histogram of Orientations

**VMF** Vector Median Filter

**WLS** Weighted Least Squares

**MLS** Moving Least Squares

**ROS** Robot Operating System

**GPS** Global Positioning System

# I. INTRODUCTION

In these days, autonomous cars are the most exciting and important topic of the automotive industry. It is expected that the future cars will be autonomous, which don't need to any human for vehicle operations. In this way, ninety percent of the traffic accidents caused by human error and deaths in these accidents will be avoided. Additionally the traffic congestion can be prevented, as well as the substantial reduction in fuel consumption and environmental pollution caused by vehicles will be achieved. In addition, it is thought that with driverless cars, which enables the elderly or disabled people to move more easily, may have effects that facilitate social life and bring balance.

Looking at the history of autonomous vehicles, the first radio-controlled vehicle is introduced in 1925 by a company called Houdina Radio Control. Then, in 1956, the Firebird vehicle of General Motors went on the highway automatically, reading the signals from the radio transmitters installed on the road. After a short period of two years, the Chrysler company Imperial model vehicle for the first time is used cruise control. The first models that could travel on their own are introduced in the 1980s. The first vehicle which has applied computer vision, sensors and high-speed processors to create vehicles that drive themselves, is built in 1984 with the Navlab and ALV projects of Carnegie Mellon University. In the 90s, technological innovations such as anti-lock braking system (ABS) which prevents slipping and skidding during braking, cruise control system that keeps the vehicle constant at the determined speed in 2000s and automatic parking assistant are developed. These are technologies that supported drivers, but systems where cruise control was still human [1].

Since 1987, numerous large companies and research organizations have worked on driverless vehicles including Mercedes-Benz, General Motors, Bosch, Nissan, Toyota, Volvo, Mitsubishi, Renault, Audi, Peugeot, Tesla Motors and Google each exhibited different prototypes [2–10]. In 2002, a competition organized by the American DARPA

agency began to provide funding for autonomous vehicles [11]. In 2009, Google announced the launch of its first driverless vehicle project [12]. In June 2010, a Linea model vehicle has been equipped with a LIDAR, an electric steer, brake and an electronic card to control the throttle through CAN Bus. An obstacle avoidance program were developed and this autonomous vehicle were tested successfully at Okan University Campus in June 2011 [13]. In July 2013, Vislab demonstrated BRAiVE, a vehicle that moved autonomously on a mixed traffic route open to public traffic [14].

Autonomous vehicles will bring some dangers and disadvantages with the ease and advantages it brings to human life. The vehicles will need to be connected to the internet to communicate with other vehicles (V2V) and infrastructure protocol (V2I) and this will facilitate the means of hacking [15]. Moreover, it will be a great convenience for terrorist attacks because of their full autonomy and remote control capability.

Apart from these, there are still some problems about ethical and moral reasoning. There are, for example, contradictions as to whether the vehicle will hit the bus in an inevitable collision or if it breaks in another direction, risking possible pedestrians or passengers in the vehicle. Even taking a decision on an imminent fatality between two animals is very important moral issue.

In 2016, the Google Driverless Vehicle made its first accident [16]. In the same year, a Tesla car crashed while in driverless mode and the driver lost his life [17]. This is the first fatal accident involving a driverless vehicle. However, an incident in 2018 was the first accident in which a driverless vehicle caused the death of a pedestrian [18].

In recent years, autonomous vehicles capable of traveling without human intervention in automotive technology have been the last point in the light of intelligent systems and have been able to successfully accomplish almost all tasks in controlled environments.

Thanks to the automatic control systems in autonomous vehicles in good weather conditions, it can detect road, traffic signs, traffic flow and environment without the need of driver and travel without the intervention of the driver. Autonomous vehicles can detect objects around them using technologies and techniques such as radar, LIDAR, camera, GPS, odometer, computer vision. But the most challenging situation for autonomously moving vehicles is adverse weather conditions. Those conditions like foggy, snowy, rainy corrupt the data from the sensors and causes noise. Sensors that allow autonomous vehicles to move on their own in adverse weather conditions, as with the same people, have difficulty in providing accurate data.

### **1.1. Literature Review**

With the progress of technology and the introduction of autonomous vehicles into our lives more and more, the number of academic studies on the performance of autonomous vehicles is increasing. Even when driving in a man-controlled vehicle, adverse weather conditions are very challenging and dangerous to human vision. This also applies to autonomous vehicles. Especially in adverse weather conditions, many autonomous vehicles use multiple sensors to detect obstacles and support the navigation system such as cameras, LIDAR, radar, sonar. The performance of these sensors in weather conditions such as rain, fog, snow and hail is not at the desired level and this situation makes the autonomous movement ability very difficult. Therefore, especially for autonomous vehicles, it is important to study on improving the performance of these sensors. In this section, studies on improving the performance of sensors used in autonomous vehicles in adverse weather conditions are examined in the literature.

A comprehensive literature survey on the effects of bad weather on sensors commonly used in autonomous vehicles such as LIDAR, radar, camera and GPS is provided in [19]. A useful study has been made to summarize the responses of each sensor in different weather conditions and summarize the studies on these subjects. They also



characterized the effects of rain on millimeter-wave (mm-wave) radar.

In [20], LIDAR can identify objects superior to other sensors, especially in adverse weather. In this study, a neural network technique which is used to detect the weather by fusion with LIDAR and camera sensors is proposed in order to automatically adjust the vehicle speed depending on the weather.

Upon the effect of LIDAR sensor on weather conditions, theoretical study is analyzed in [21] based on LIDAR sensor and fog, snow, rain weather phenomena based on physical principles and prediction of effects. In this theoretical study, mathematical formulas of the extinction coefficients of LIDAR rays and the varying backscatter coefficients in adverse weather conditions are presented according to the distribution of particle diameters and snowfall/rainfall precipitation ratios for each weather situation. In addition, electro-optical laser radar target simulator is produced to test sensor performances and laser radar performance in foggy environment is simulated.

In [22], order to give a vision to the studies related to autonomous vehicles and adverse weather conditions, various sensors are operated in an outdoor environment for a long time to understand what is happening in adverse weather conditions with the test results are emphasized. In general, radar is used for driving functions, optical sensors are used for distances of 100-400 meters, and at least two distance sensors, such as radar and LIDAR, have to be used.

Ultra-Wideband (UWB) Radar and LIDAR sensors are compared with the tests in [23]. Tests are performed in artificial fog environment by mounting LIDAR and UWB Radar on the robot. When the results are analyzed, in dense foggy environments it is observed that the vision of LIDAR is reduced to less than 1 meter and UWB radar has the same vision like in the clean air. UWB Radar has been advocated that it is not affected by adverse weather conditions and that LIDAR is not efficient. In the open air, it is emphasized that UWB Radar has less resolution than LIDAR and that LIDAR will

always provide more sensitivity.

2D LIDAR data is applied in five and seven dimensional Median Filters in two stages, from right to left and in time space in polar space and a study that is claimed to be successful [24]. In this study, it is argued that the distribution of the snowflakes detected by gamma distribution can be explained. Information is also given on how LIDARs, pulsed laser scanners, detect snowflakes. LIDAR sends laser pulses and scattering occurs when a laser beam hits snowflakes. Some of the emitted light is reflected back to the detector, and if the pulse is strong enough, the detector is triggered and the range can be calculated.

In adverse weather conditions, the quality of the sensors and the detection conditions are also very important. In [25], four different LIDAR sensors are tested during six different snowfalls and their behavior is characterized. It is emphasized that one of the most important features among sensors is the echo number and the other is the wavelength of the laser beams of the sensors.

On the snow and wet road surfaces, the LIDAR point cloud is disrupted by the reflection of the LIDAR rays hitting the wet ground. In [26] and [27], the structure and density modeling of the map images in the vehicle location is reconstructed the accumulated LIDAR image using Principal Component Analysis (PCA). Also, the edge profile matching method is used to reduce the effects of snow lines on the edge profiles of LIDAR and map images, and to estimate the lateral position of the vehicle and to reduce its lateral uncertainty. When testing these methods on a real car, it has been argued that the lateral error is reduced to 20 cm when traveling at a speed of 60 km / h and the error is reliable for autonomous movement.

Using 3D point cloud data from 3D LIDAR, a study to filter snow noise in snowy weather is investigated in [28]. Existing 2D and 3D noise reduction studies and filters are explained in detail and even a 2D filter has been tested as an example, due to the

small number of studies performed in the literature to remove snow noise from LIDAR data during snowfall. It is argued that Radius Outlier Removal (ROR) filter is the best cleaning filter for snow noise in 3D point cloud filters which is the main focus of the article. However, it has been found that ROR filter also eliminates important environmental features at long distances, i.e. objects become sparse as they move away from LIDAR. This is considered to be a major problem in autonomous driving, especially since LIDAR is needed for localization, object detection and planning. As a result, the Dynamic Radius Outlier Removal (DROR) filter algorithm is developed. It has also been advocated that the DROR filter eliminates more snowflake after three meters from LIDAR compared to the ROR filter.

The electronic Signal to Noise Ratio (SNR) has performed using formulas of collected power from the background (using LIDAR equation), detected photocurrent signal intensity out of detector and responsivity of detector [29]. Also, extinction and backscattering coefficients of adverse weathers has analyzed which are ( $5 \times 10^{-3}$  to  $1, 5 \times 10^{-3} m^{-1}$ ) for fogs, ( $10^{-3}$  to  $5 \times 10^{-3} m^{-1}$ ) for snowfalls and under ( $10^{-3} m^{-1}$ ) for rainfalls.

LIDAR is an optical sensor for detecting the distance or surface of the objects around it. LIDAR uses light differently than radar, which operates in a similar way and uses radio waves. The method used is to estimate the distance after sending pulsed laser light to the target, measuring the reflected pulses with a sensor, and with respect to the flight time of the light. 3D LIDARs are often used for three-dimensional scanning and mapping. LIDAR's are characterized by their scan frequency (maximum scanning speed), horizontal angle (maximum scanning angle), range (maximum measurement distance), resolution (minimum angle between two consecutive measurements) and number of layers (number of simultaneous scanning planes) [30].

In [31] and [32], LIDAR has a much smaller wavelength than radar. This shows that

LIDAR has a higher spatial resolution, which means that it can perform 3D scanning of targets such as buildings, bridges and rock, unlike radar. Another advantage of LIDAR is that laser beams can detect targets at very long distances with very low error rates. The disadvantage of such a low wavelength is that it is difficult to detect small water vapor particles in adverse weather conditions such as fog, snow, rain and snow.

A study to detect the presence of rain or snow is given in [33]. In this study, Gauss Mixture Model is used to differentiate the foreground of dynamic weather events from the background. The Histogram of Orientations (HOS) of rain or snow streaks is calculated based on photometry and size to detect rain in the foreground extracted.

Especially for snowfall, the snowfall rendering methods in simulation environment are presented in [34–37] by considering their physical properties.

In [38], it is argued that the snowflakes are destroyed by using Median Filter according to the speed and size of the moving particles from the images recorded through the camera. It is reported that the study also destroyed small and moving objects and failed in heavy snowfall.

In order to eliminate Gaussian, impulse, speckle noises in the reflected signal from the target, an mean filter algorithm that fused LIDAR intensity and range data is investigated in [39].

The  $\lambda/\mu$  filtering algorithm, which uses the Mean Shift method to parse the full waveform data of LIDAR, is proposed in [40].

A new noise reduction algorithm for Adaptive Mean Filter (ADMF) has been developed for the full waveform LIDAR signal [41]. According to the tests performed in the study, the high contrast and signal-to-noise ratio of the ADMF has been advocated to be more efficient than the median and mean filters and very suitable for reducing noise.

A universal de-noising algorithm for LIDAR has been studied on the basis of signal segmentation and reconstruction [42].

The properties, theoretical analysis and applications of the median filter are mentioned in [43–45]. The median filter is used to eliminate salt and pepper noises in the image and averaged neighboring pixels to improve in [46]. Other studies on the median filter, as an image-processing technique, where noise is tried to be eliminated and compared to other filters are shown in [47] and [48]. The vector median filter (VMF) is described in [49] and the noise reduction method using VMF is presented in [50].

In addition, a number of studies are performed that use and describe the least mean squares filter [51–53]. The adaptation to very quick changes in signal characteristics is described in [54] to cancel noise and predict future implementation. The local least squares approach to scattered data for the linear system equations and derived weighted least squares (WLS) and moving least squares (MLS) methods are presented in [55]. Also a weighted least squares algorithm used for time-of flight depth image de-noising is shown in [56].

## **1.2. Hypothesis**

According to the studies conducted in the literature, there are some published material that characterize the particles of weather events such as fog, snow, rain and hail in adverse weather conditions. However, there are very few studies aimed at improving sensor vision, especially in these weather conditions. In some articles, median filter has been used to improve sensor data. However, the median filter is particularly effective in improving noise in a single frame or picture. It will distort the image too much in an environment with real-time and moving objects. While most of the studies examined focused on snow, it is found that it is mostly worked under light snowfall and from a fixed point.

In this thesis, based on the aforementioned issues, De-noising algorithm improved by Least Mean Squares Filter for autonomous vehicles in snowfall, has been developed. This algorithm can be used effectively in a vehicle under heavy snowfall and in real time, can remove noise such as snowflakes and try to estimate objects which are behind the snowflakes while removing these noises.

### **1.3. Outline of Thesis**

The thesis is organized as follows. In the second chapter, the filters and the methodology used to develop the de-noising algorithm are described. In addition, the necessary tools for testing the developed algorithm are mentioned. In the third chapter, the experimental results on a autonomous vehicle are mentioned. Finally, chapter four describes the conclusion.

## II. DE-NOISING ALGORITHM DEVELOPMENT & METHODOLOGY

To study on noise-causing snowflakes, data collection is required using a LIDAR sensor in snowy weather. In order to collect data from LIDAR, required to the Nvidia Jetson TX1 developer kit, which is frequently used in autonomous vehicles and runs autonomous machine software quickly, with less power, needed performance and power efficiency. Robot Operating System (ROS) platform is used to communicate with the sensor and hardware and to record data from LIDAR connected to the Jetson card. The data recorded with ROSBAG command is worked on MATLAB and filtered. In Fig. 2.1., the diagram describing these operations is shown.

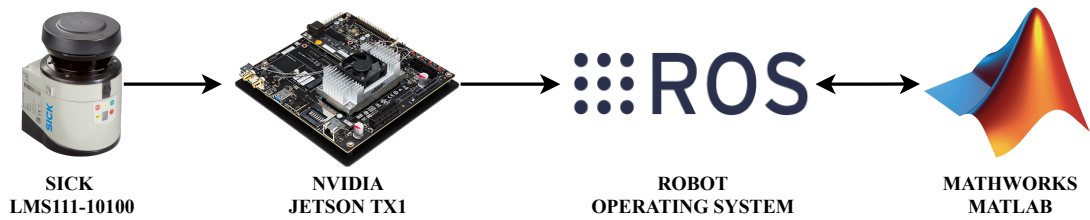


Fig. 2.1.: Connection of Tools

### 2.1. Tools

#### 2.1.1. Laser Imaging Detection and Ranging

LIDAR is a device for measuring distance using laser beams. The range calculation to measure how far laser beam has travelled to and from an object, is given in Equation (2.1) from [57].

$$Distance = \frac{(Speed\ of\ Flight) * (Time\ of\ Flight)}{2} \quad (2.1)$$

In this study, SICK LMS111-10100 (shown in Fig. 2.2.) are used as a LIDAR, which is designed to work both in indoor and outdoor environment [58]. The LMS111 is a 2D laser measurement sensor that scans its surroundings. Using a laser diode and a

rotating mirror, it emits infrared laser pulses with a wavelength of 905 nm. It measures reflected laser pulses within the angular range of 270°. Information on the features and performance of the LMS111-10100 [59] are given in Table 2.1. and Table 2.2.



Fig. 2.2.: LIDAR (SICK, LMS111-10100)

Table 2.1.: Features of LMS111-10100

Application	Outdoor
Light source	Infrared (905 nm)
Laser class	1 (IEC 60825-1:2014, EN 60825-1:2014)
Aperture angle	Horizontal 270°
Scanning frequency	25 Hz / 50 Hz
Angular resolution	0.25°/ 0.5°
Heating	Yes
Working range	0.5 m ... 20 m
Scanning range	18 m (At 10% remission), 20 m (At 90% remission )
Amount of evaluated echoes	2
Fog correction	Yes

Table 2.2.: Performance of LMS111-10100

Response time	$\geq 20$ ms
Detectable object shape	Almost any
Systematic error	$\pm 30$ mm
Statistical error	12 mm
Integrated application	Field evaluation with flexible fields
Number of field sets	10 fields
Simultaneous evaluation cases	10



The LMS111 sends a laser pulse to each degree of scanning ( $0.25^\circ$  or  $0.5^\circ$  depending on resolution) and waits for it to be reflected back. If the laser pulse strikes an object within the measuring range (20 meters), it is reflected back to the loss. LIDAR measures the time between the outgoing and incoming pulses and determines the distance of the object according to this difference. Working range diagram of LMS111 [59] shown in Fig. 2.3.

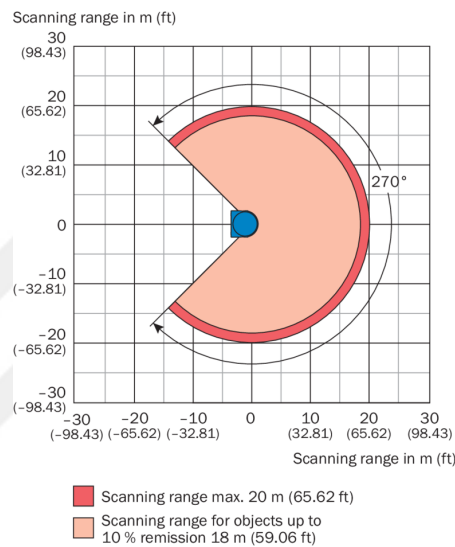


Fig. 2.3.: Working Range Diagram of LMS111-10100

The LMS111 can analyze two echo signals for each measuring beam. This enables it to provide reliable measurement results at all times even if it is behind glass or exposed to adverse weather and environmental influences outdoors [60]. Filters providing this Multi-Eco Technology are switched off for study.

### 2.1.2. NVIDIA - Jetson TX1 Developer Kit

Nvidia Jetson TX1 Developer Kit shown in Fig. 2.4. which is a full-featured development platform for artificial intelligence programming designed for high performance and speed. Technical specification of Jetson TX1 [61] is given in Table 2.3.

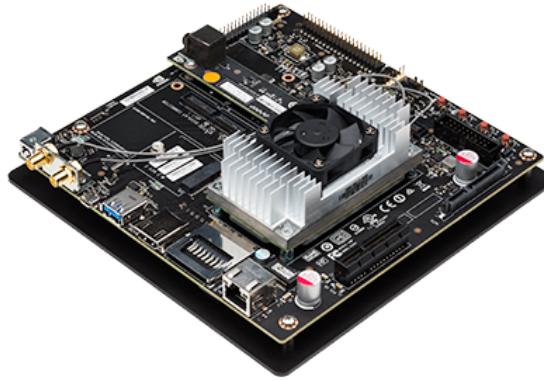


Fig. 2.4.: Nvidia Jetson TX1 Developer Kit

Table 2.3.: Technical Specifications of Nvidia Jetson TX1 Developer Kit

GPU	NVIDIA Maxwell with 256 NVIDIA CUDA Cores
CPU	Quad-core ARM Cortex A57 MPcore
Memory	4 GB LPDDR4
Storage	16 GB eMMC 5.1
Connectivity	Connects to 801.11ac WLAN and Bluetooth
Camera	5 MP MIPI CSI
Display	HDMI

### 2.1.3. Robot Operating System

ROS is an open-source, meta-operating system. It provides hardware abstraction, low-level device control, implementation of commonly-used functionality, message-passing between processes, and package management. It also provides tools and libraries for obtaining, building, writing, and running code across multiple computers [62].

For this study, mostly "roscat" [63] and "lms1xx" [64] packages are used. Roscat package used for recording and playing Ros Topics. LMS1xx package is ROS driver for Sick LMS1XX LIDARs and used for get datas from sensor.

## 2.2. Proposed De-Noising Algorithm Approach

### 2.2.1. Median Filter

Median filter is a popular non-linear noise reduction technique that is frequently used in signal and image processing. It is particularly effective in removing random noises

such as impulse or salt-pepper. It is a good alternative to linear filters due to the ability to protect the edges of the signal or image while eliminating noise.

The Median Filter is mainly useful for reducing noise by smoothing images or signals. It can maintain discontinuity and smooth noise without affecting surroundings.

As used in this study, the one-dimensional (1D) Median Filter takes the points inside a  $2N + 1$  length window and begins to shift the window as small as the filter size. Median Filter is applied separately in each small window. This is done by sorting the values within the small window from small to large, and then retrieving the median as a result. The formula of the Median Filter is given in Equation (2.2) from [45].

$$y(k) = \text{med}\{x(k - N), \dots, x(k - 1), x(k), x(k + 1), \dots, x(k + N)\} \quad (2.2)$$

### 2.2.2. Least Mean Squares Filter

Least Mean Squares (LMS) Filter is the most popular adaptive filter with its simplicity and ease of application. It is particularly suitable for signal processing and is the first filter of choice for real-time systems, as it requires less computation than other adaptive filters. It does not require any information about the statistical properties of the environment, so it is robust in the face of unknown environmental influences.

Adaptive filter should be used for fast convergence and low mean square error [65]. They are digital filters with features that adjust filter parameters to accommodate changing signal characteristics at the input. They adapt quickly and automatically to changes in the input signal.

Discovered by Bernard Widrow and Ted Hoff in 1960, the LMS filter continuously updates the output to filter weights. At first, all coefficients in the filter are set to an initial value. The filter output is then calculated using the available coefficients. Estimation error is calculated according to the estimated output and the coefficients are updated by returning to the beginning. LMS filter formulas are given in Equation (2.3), Equation

(2.4) and Equation (2.5) from [66].

$$(X_1, Y_1), (X_2, Y_2), \dots (X_n, Y_n) = (X_i, Y_i) = (time, range) \quad (2.3)$$

$$\hat{Y} = a + bX \quad (2.4)$$

$$\epsilon = \sum_{i=1}^N (Y_i - \hat{Y}_i)^2 = \sum_{i=1}^N [Y_i - (a + bX_i)]^2 \quad (2.5)$$

### 2.2.3. Proposed Method

In order to determine how often snowflakes appeared in LIDAR data and to study them, it is necessary to record in a snowy weather. Therefore, initial data are collected on Sunday, 24 February 2019, which is shown in Fig. 2.5., via the LIDAR sensor in real snow. Data from the LIDAR sensor is plotted using the Robot Operating System (ROS) on the NVIDIA Jetson TX1 card and recorded as a bag file (rosbag). Then, the recorded data are processed by MATLAB and various studies are performed. As a result of these studies, improvements are made to filter out undesirable particles such as snowflake against adverse weather conditions which are problematic in LIDAR and similar sensors which enable mapping or object detection for autonomous systems to act on their own.



Fig. 2.5.: Sunday, 24 February 2019 - Snowfall

First, the data structures are edited using the MATLAB library to make the bag file transferred to MATLAB ready for filtering. Then, how often and how snowflakes appeared in the LIDAR data obtained in snowy weather are examined. As a result of this examination, it is determined that the distance of snowflakes showed very sudden changes when compared with the distance of other objects around. Considering this situation, it is provided to determine the points causing the sudden change between the ranges (t) and (t-1) by using the threshold value.

$$r(k, t) - Ranges(k, (t - 1)) < TH \quad (2.6)$$

In Equation (2.6),  $r(k, t)$  is the range data from LIDAR, which is currently received (t moment) and not yet processed.  $Ranges(k, (t - 1))$  is the range data from LIDAR, which was filtered and stored at the previous moment (t-1).

In case the detected point was an object moving in the frame, (t-2), (t-3) moments of the current points are checked additionally which is shown in Equation (2.7).

$$r(k, t) - r(k, (t - 1)) < TH \quad \& \quad r(k, t) - r(k, (t - 2)) < TH \quad \& \quad r(k, t) - r(k, (t - 3)) < TH \quad (2.7)$$

For example, the moving object that enters the frame with a sudden change at (t) will be considered as noise and removed. However, due to the fact that some historical data is recorded, the algorithm gives the output from the moment (t + 1) instead of deleting it if (t + 1), (t + 2) and (t + 3) are similar to the value at (t). In order to detect noises such as snowflakes, if differences between the point at the time (t) and any of the points of (t-1), (t-2), (t-3) remain above the threshold value, the point in the moment of (t) is assumed to be noise. Fig. 2.6. shows flowchart showing these steps.

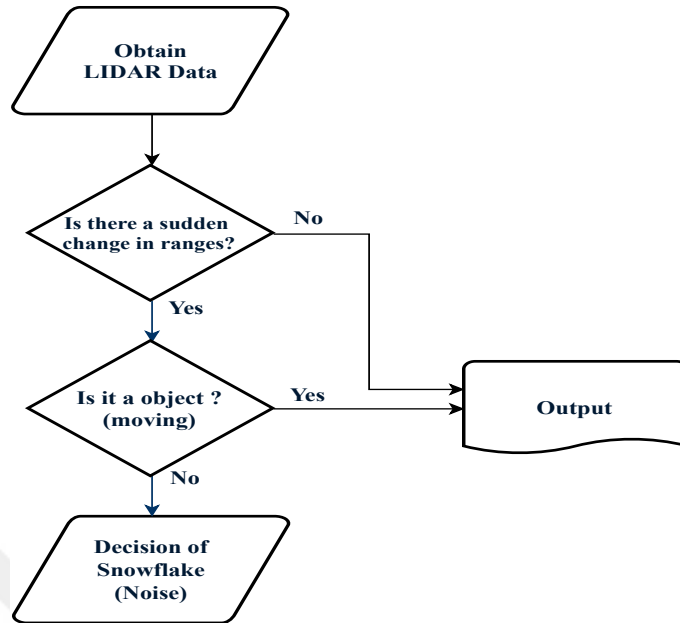


Fig. 2.6.: Noise Detection Flowchart

The next step is to remove the detected snowflakes and use the historical data to estimate the objects which are behind of snowflake, should actually be in. Used historical data is given in Equation (2.8).

$$Vector = [Ranges(k, (t - 1)) \ Ranges(k, (t - 2)) \ \dots \ Ranges(k, (t - n))] \quad (2.8)$$

In order to estimate objects, LMS filter, which continuously updates itself according to the input information, makes a possible prediction. The pseudocode in Fig. 2.7. that shows how this filter is integrated into the algorithm created to select noisy points.

$$y(k, t) = LMSFilter(Vector) \quad (2.9)$$

In Equation (2.9),  $y(k, t)$  is the result data obtained from the LMS filter.

As a result, the study is about detecting and filtering points that change suddenly and exceeding a certain threshold, while at the same time keeping moving objects. The proposed method is De-noising Algorithm improved with Least Mean Squares Filter. The flowchart of the final proposed method is shown in Fig. 2.8.

**Algorithm 1:** Pseudocode of Proposed Method

---

**Input:**  $r(t)$   
**Output:** Ranges( $t$ )  
**for**  $t=filtersize:LastFrame$  **do**  
  **for**  $k=1:541$  **do**  
    **if**  $r(k,t)-Ranges(k,(t-1))<TH$  **then**  
       $plot\_r=r(k,t);$   
    **else if**  $r(k,t)-r(k,(t-1))<TH \ \& \ r(k,t)-r(k,(t-2))<TH \ \& \ r(k,t)-r(k,(t-3))<TH$   
      **then**  
         $plot\_r=r(k,t);$   
    **else**  
      Vector= [ Ranges( $k,(t-1)$ ) ... Ranges( $k,(t-n)$ ) ];  
      result= LMSFilter(Vector);  
       $plot\_r=result;$   
    **end**  
  **end**  
 Ranges( $k,t$ )= $plot\_r;$   
**end**

---

Fig. 2.7.: Pseudocode of Proposed Method

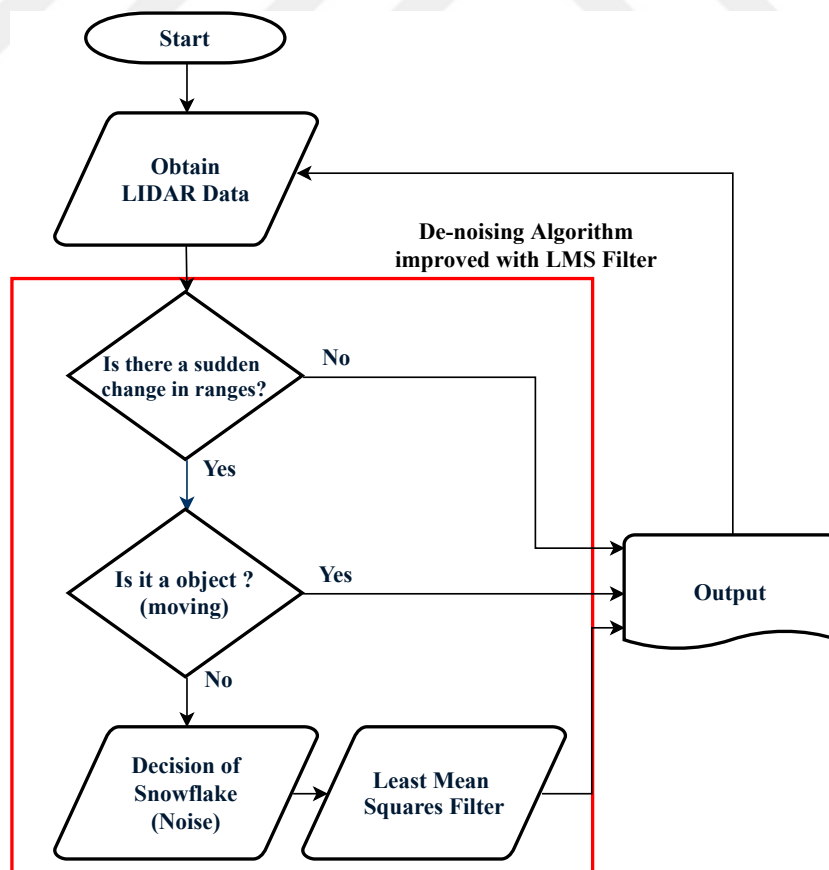


Fig. 2.8.: Flowchart of De-Noising Algorithm Improved with Least Mean Squares Filter

### III. EXPERIMENTAL RESULTS

This section describes the experimental results. The first record which is in snowy weather, used to understand snowy conditions and improve the algorithm for these conditions. All following experimental results are obtained with Autonomous Research Vehicle OKANOM, which is performed by Istanbul Okan University UTAS Center in 2012 [13]. OKANOM which is shown in Fig. 3.1., is a second level autonomous ground vehicle that can move from place to place without any external intervention by using the route it creates with the position information it receives via GPS.



Fig. 3.1.: Autonomous Research Vehicle, OKANOM

In order to observe experiments at different snow densities and insufficient snowfall in the city, an artificial snow machine with 1500 Watt power, which can be adjusted to different snow throwing densities, is purchased and the test environment is created. LIDAR is fitted with a weather protection cover with an angle of 190° to prevent any damage. In Fig. 3.2., there is a representative photograph of working of the snow machine.





Fig. 3.2.: Artificial Snowfall

The first record which is taken on snowy weather on Sunday, February 24, 2019, consists of a total of 24777 frames. The first frame of this record plotted on MATLAB is as in Fig. 3.3. The transition between each frame is 0.02 seconds and therefore the total recording is 8.26 minutes. In order to determine how much snowy points (noises) exist in this 24777 frame and to understand how effective the applied filters are, where the noisy points are formed, this area is selected as a polygon. With the selected area, the number of points inside and outside the area is checked. Fig. 3.3. shows the frame with the highest noise (11 points) among the 24777 frames and in Fig. 3.5. the polygonal method is applied to this frame and the points are marked. When all the recorded data are checked in this way, it is found that there were 7312 unwanted points in the total of 24777 frames and approximately 0.3 snowflakes per frame. This proves that snowfall is very rare and slow (or that some of the snowflakes are too small to be detected by the LIDAR sensor).

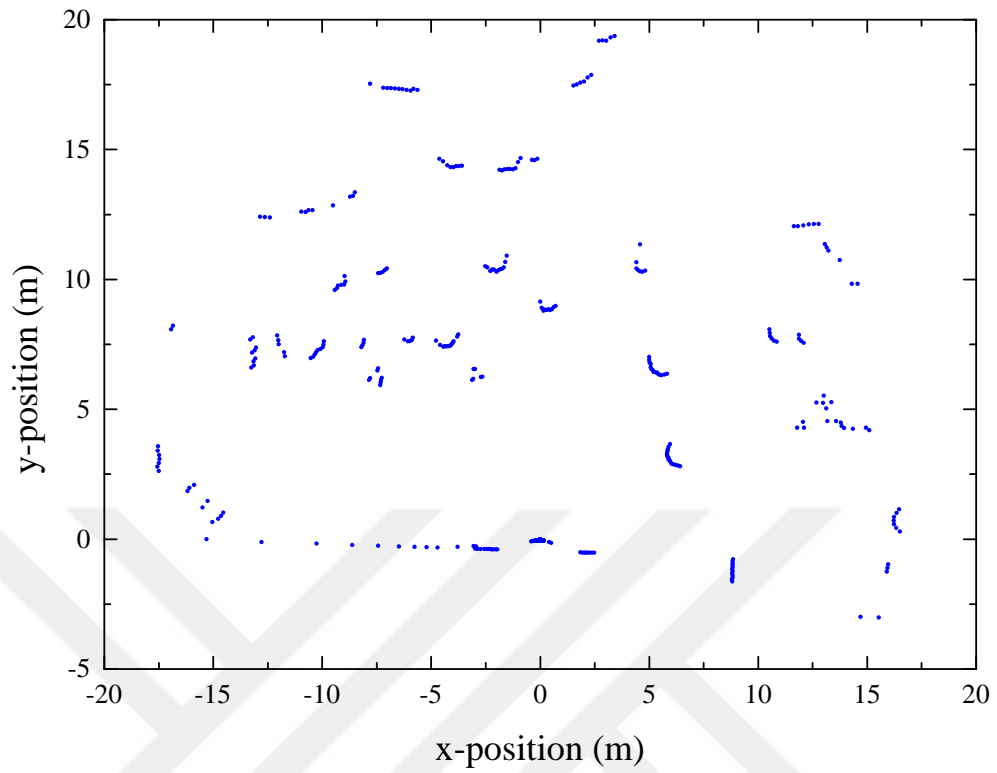


Fig. 3.3.: First Frame of Snowy Weather

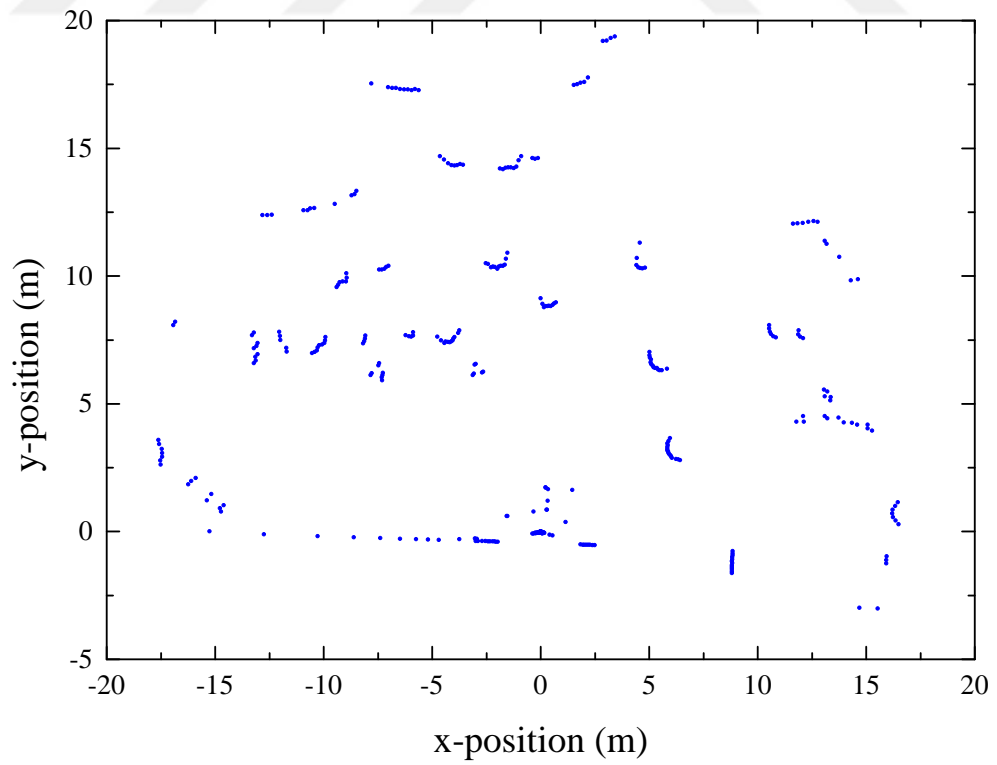


Fig. 3.4.: The Highest Noisy Frame of Snowy Weather

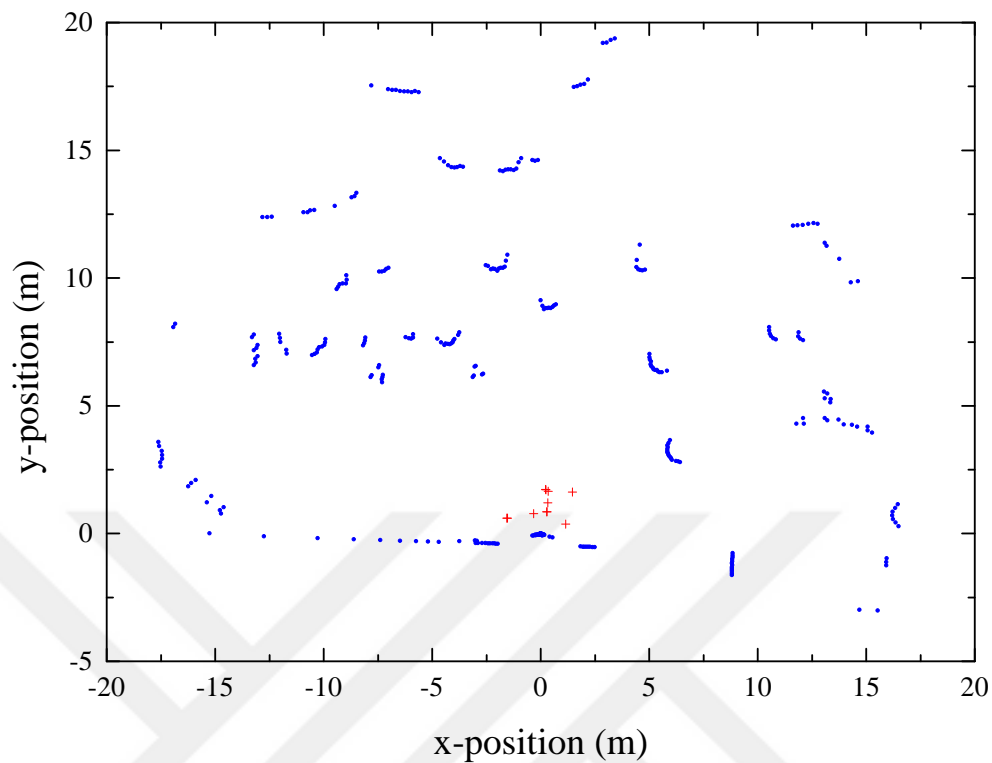


Fig. 3.5.: Marked Noisy Frame of Snowy Weather

Various existing filters have been tested to eliminate noisy points and algorithm has been developed based on these results. The median filter used to eliminate noise in a picture frame and the LMS filter, which is an adaptive filter also used to eliminate noises, do not perform very well when used in an environment with moving objects. Using these filters alone causes image distortion and badly removing unwanted points. The mentioned before and developed algorithm is to identify only distances that vary greatly from a sudden and certain threshold value as noise, clearing selected noises and estimating objects behind the noises with the LMS filter and at the same time keeping moving objects.

Table 3.1. shows the recorded sensor data and the results of the applied filters. All filters worked very well as snow was sparse. In Median Filter (5) and Median Filter (15), the numbers 5 and 15 indicate the filter size. These filters are processed for all points in the frame by navigating from the current time to the points before the filter size.

Although they were good, they caused some deterioration of the original frames and greatly extended the time per frame due to the multiplicity of processing. De-noising filter is the main algorithm developed. In this filter, an algorithm is created for detecting points that change instantaneously and instead of the point where the detected noise is located, the point located in the same frame in the previous frame is placed. Although the filter gives very good results in this state, it causes some distortion when a moving object such as human enters the frame. To correct this, De-noising with LMS Filter is used. The difference of this filter from the previous one is that instead of replacing the detected noise with the point in the previous frame, it goes back to the current filter size by forming a vector and inserting this vector into the LMS filter. In this way, moving objects do not disappear and the success rate is one hundred percent. For comparison, Median Filter is used together with de-noising algorithm. The filter indicated by De-noising with Median showed 100% success due to the very rare snowfall but it took longer in terms of time than the filter installed with LMS.

Table 3.1.: Compare of Filters - Real Snow

	Original Data	Median Filter (5)	Median Filter (15)	De-noising Filter	De-noising with Median	De-noising with LMS
Total Number of Noisy Points	7312	68	0	7	0	0
Snow Density for per Frame	0.3	0.003	0	0	0	0
Success Rate (%)	-	99.1	100	99.9	100	100
Total Time (sec)	495.4	3517.5	5652.5	1320	2169.2	1837.3
Time for Each Frame (sec)	0.02	0.142	0.228	0,053	0.087	0.074

The plots of all filters shown in Table 3.1. for frame 4763 are as follows. Fig. 3.6. shows the original version of the data and there are eight unwanted points (noises).

In Fig. 3.7. and Fig. 3.8., median filters are applied directly to the original data. In Median (5) there are two noises while in Median (15) there is no noise. However, the size of the filter increases the time per frame. It also carried a few spots above the frame, although snowfall was very rare. It is noticeable when looked carefully.

In Fig. 3.10. and Fig. 3.11., the results of using De-noising Algorithm with Median Filter and LMS Filter are shown. The results are very similar due to very little snowfall. As shown in Table 3.1., both of them achieve 100% success rate. However, Median Filter is slower than LMS filter.

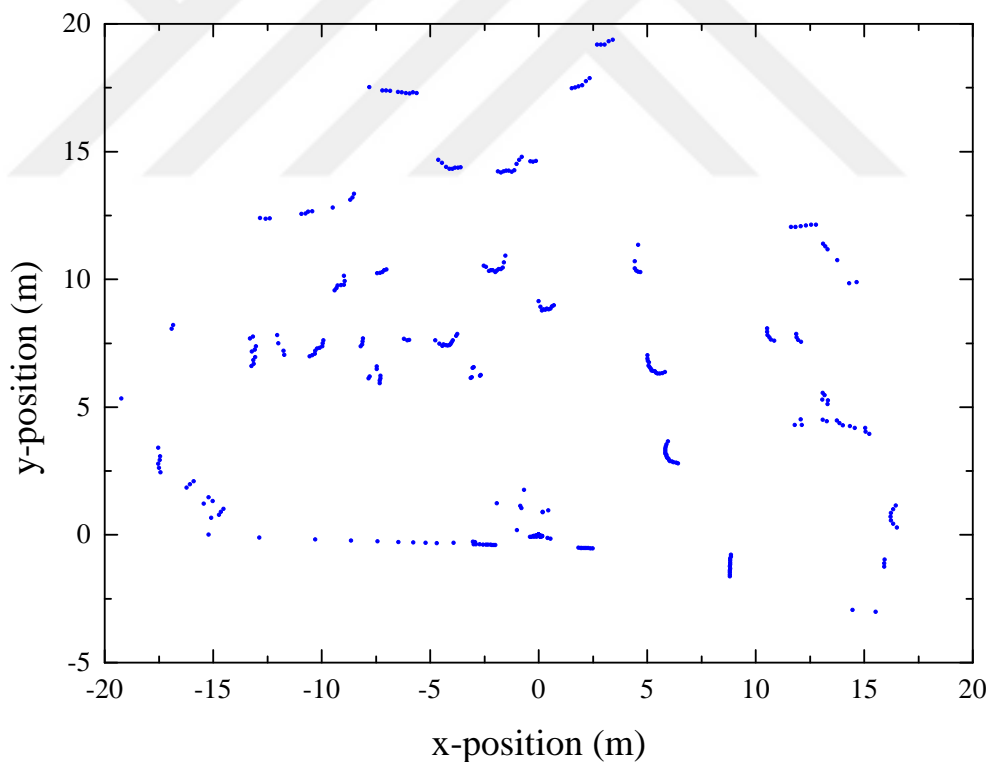


Fig. 3.6.: Original Data, (4763. Frame) - 8 Noisy Points

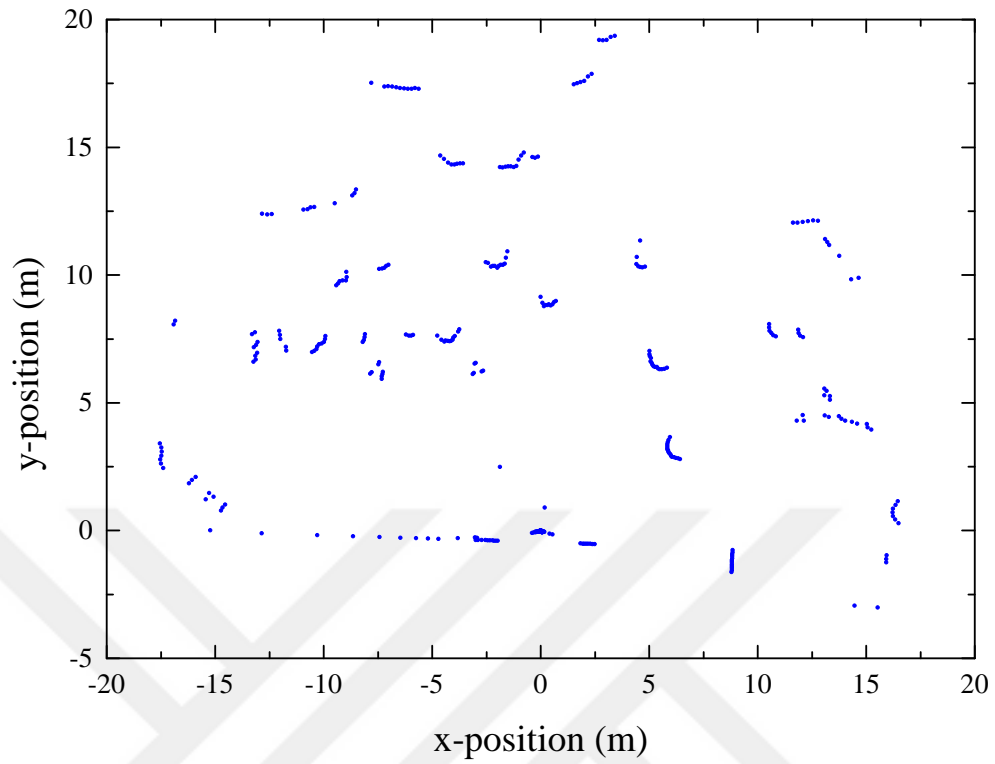


Fig. 3.7.: Median (5) Filter, (4763. Frame) - 2 Noisy Points

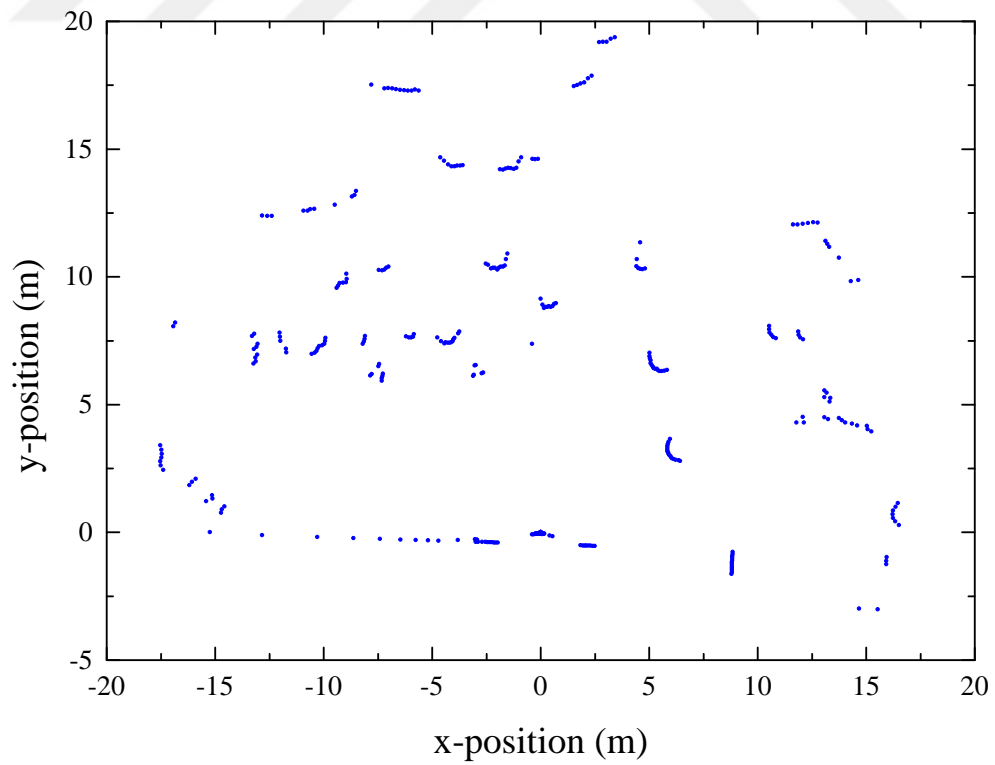


Fig. 3.8.: Median (15) Filter, (4763. Frame) - No Noisy Points

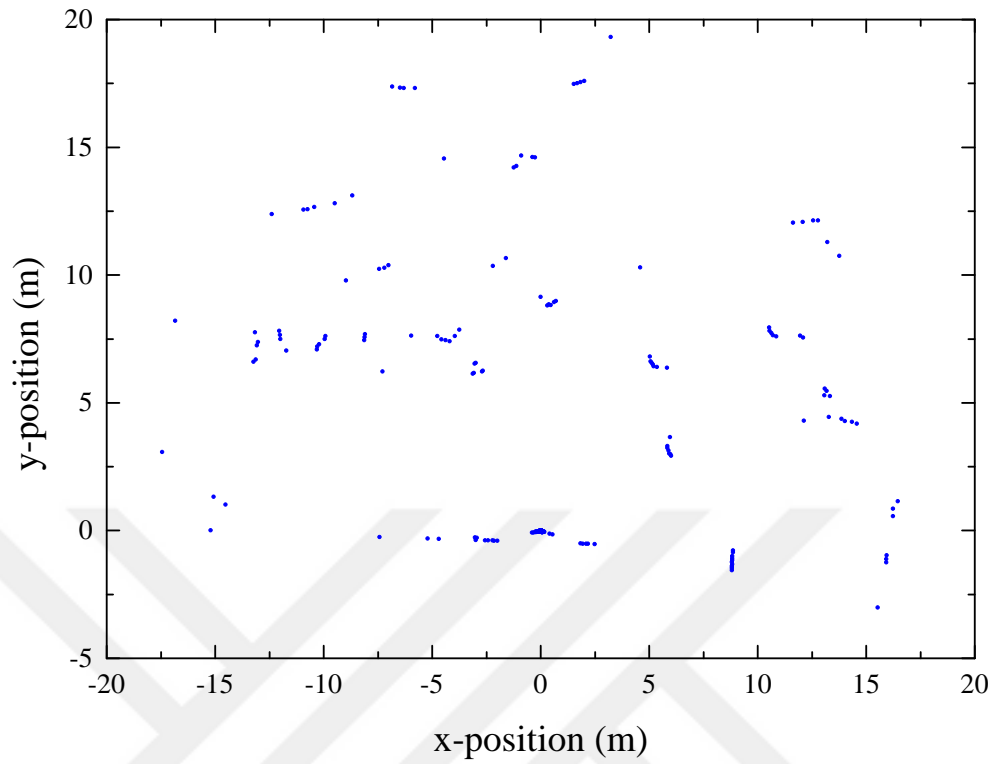


Fig. 3.9.: De-noising Filter, (4763. Frame) - No Noisy Points

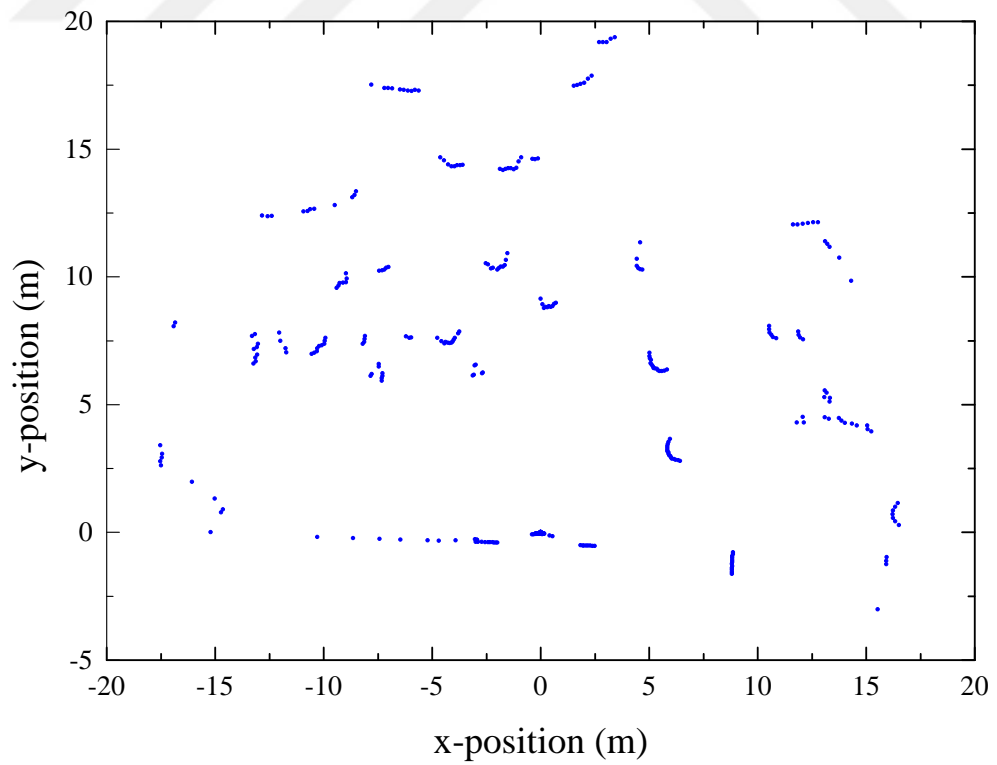


Fig. 3.10.: De-noising with Median Filter, (4763. Frame) - No Noisy Points

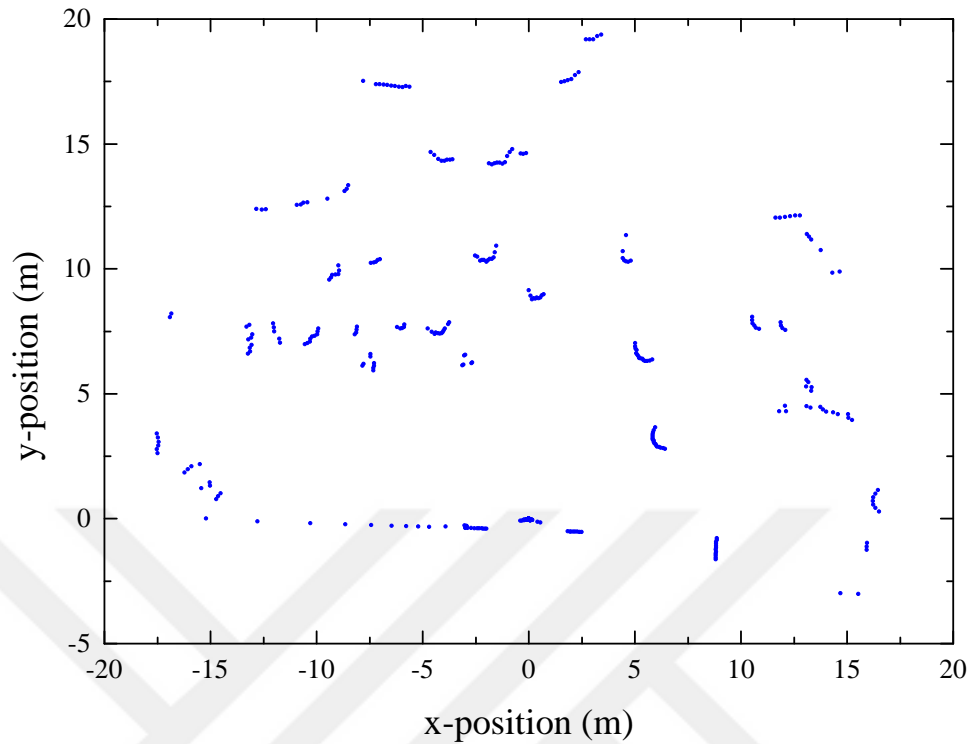


Fig. 3.11.: De-noising with LMS Filter, (4763. Frame) - No Noisy Points

A plotted version of the noise numbers in each frame of filtered and unfiltered data is shown in Fig. 3.12. Frames where noise number is zero in all filters are not plotted, and since there are too many frames in this recording, part of frames are plotted.

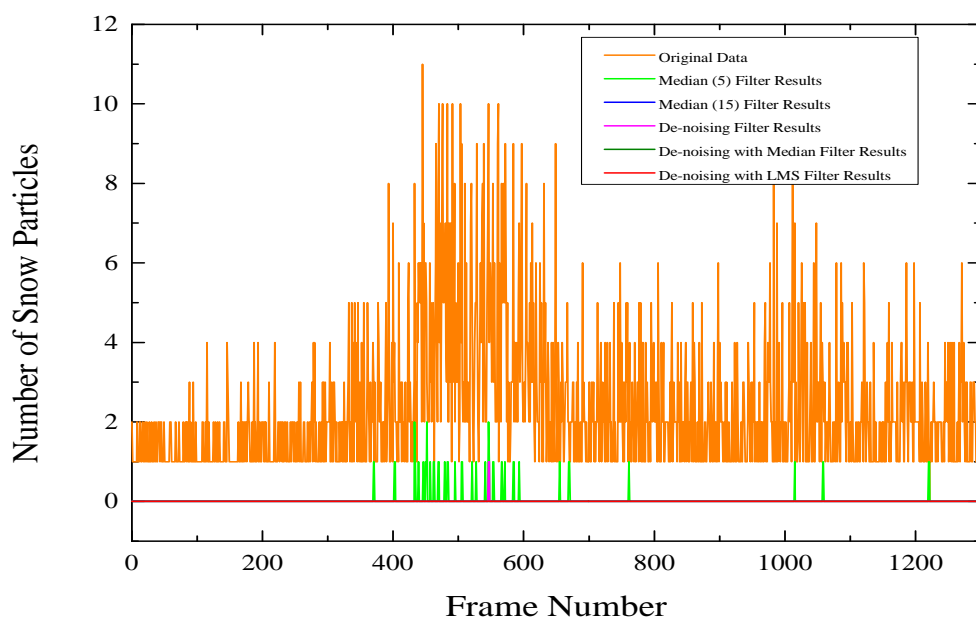


Fig. 3.12.: Noise Numbers of Frames (Real Snow)



Similar results of real snowfall conditions are also observed in tests with artificial snow. In the first artificial snow record consisting of a total of 2282 frames, 34283 snowflakes are identified in the total of all frames. Considering the time between starting and closing the artificial snow machine (2000 frames), there are 17.14 snowflake average per frame. This means that there is a heavy snowfall. Table 3.2. clearly shows that with the increase in snow density, the success rates of the Median (5) and Median (15) filters applied to the entire frame have decreased significantly. Although de-noising filter appears to be the filter that eliminates snow (noise) the most, it causes serious distortion and disappearance in the frame or moving objects. For these reasons, the values of the median and de-noising filters used alone are not taken into consideration in the tests performed hereinafter.

Table 3.2.: Compare of Filters - Artificial Snow 1

	Original Data	Median Filter (5)	Median Filter (15)	De-noising Filter	De-noising with Median	De-noising with LMS
Total Number of Noisy Points	34283	29919	20307	132	1408	144
Snow Density for per Frame	17.1415	14.9595	10.1535	0.066	0.704	0.072
Success Rate (%)	-	12.7	40.8	99.6	95.9	99.6
Total Time (sec)	45.64	129.4	132.7	58.6	66.3	63.6
Time for Each Frame (sec)	0.02	0.057	0.058	0.026	0.029	0.028

Fig. 3.13. shows the original version of the data and there are 34 unwanted points(noises). In Fig. 3.14. and Fig. 3.15., median filters have shown. There are lots of snow particles still. Disturbances in the de-noising filter which is shown in Fig. 3.16., are clearly visible when compared to the original data.

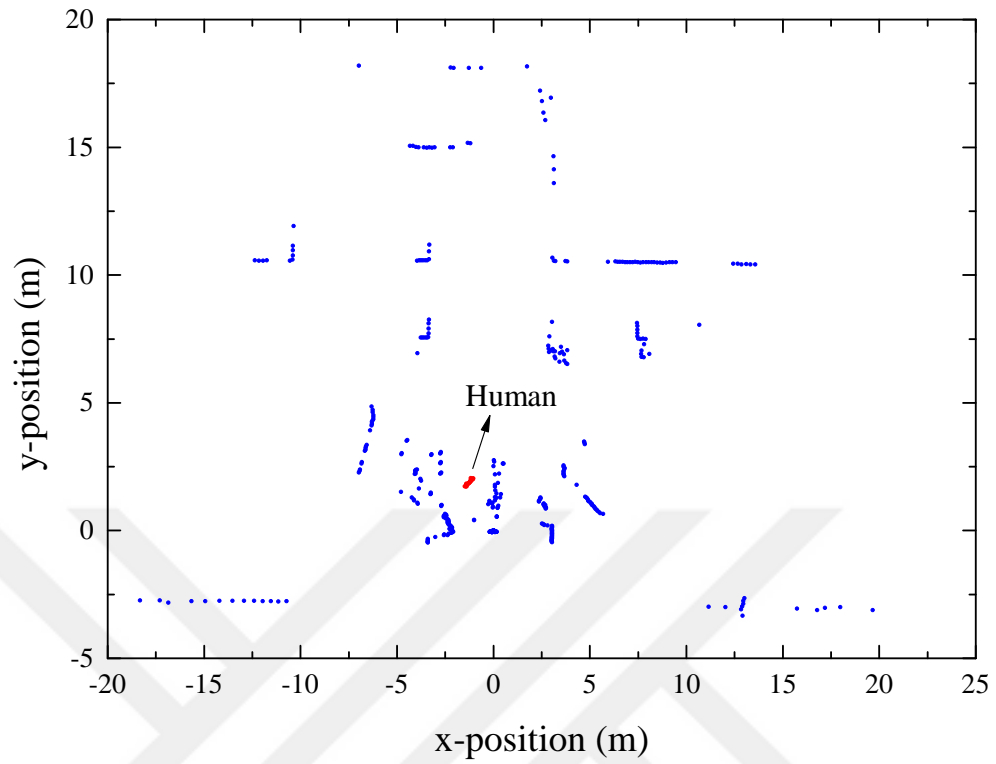


Fig. 3.13.: Original Data, (1634. Frame) - 34 Noisy Points

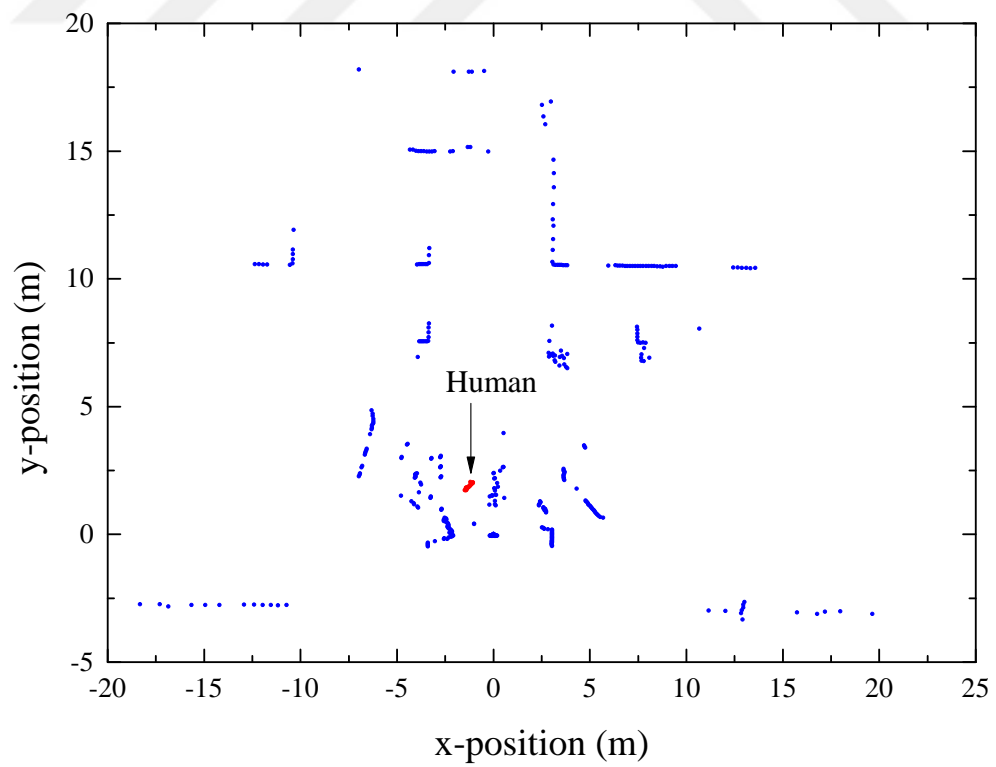


Fig. 3.14.: Median (5) Filter, (1634. Frame) - 24 Noisy Points

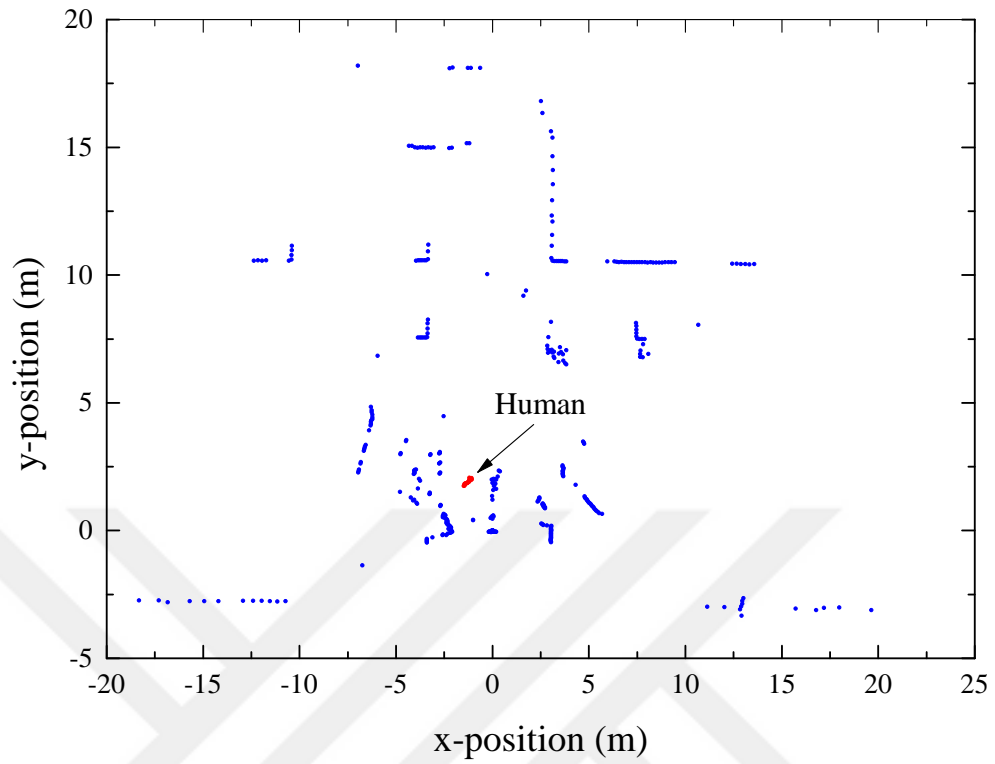


Fig. 3.15.: Median (15) Filter, (1634. Frame) - 16 Noisy Points

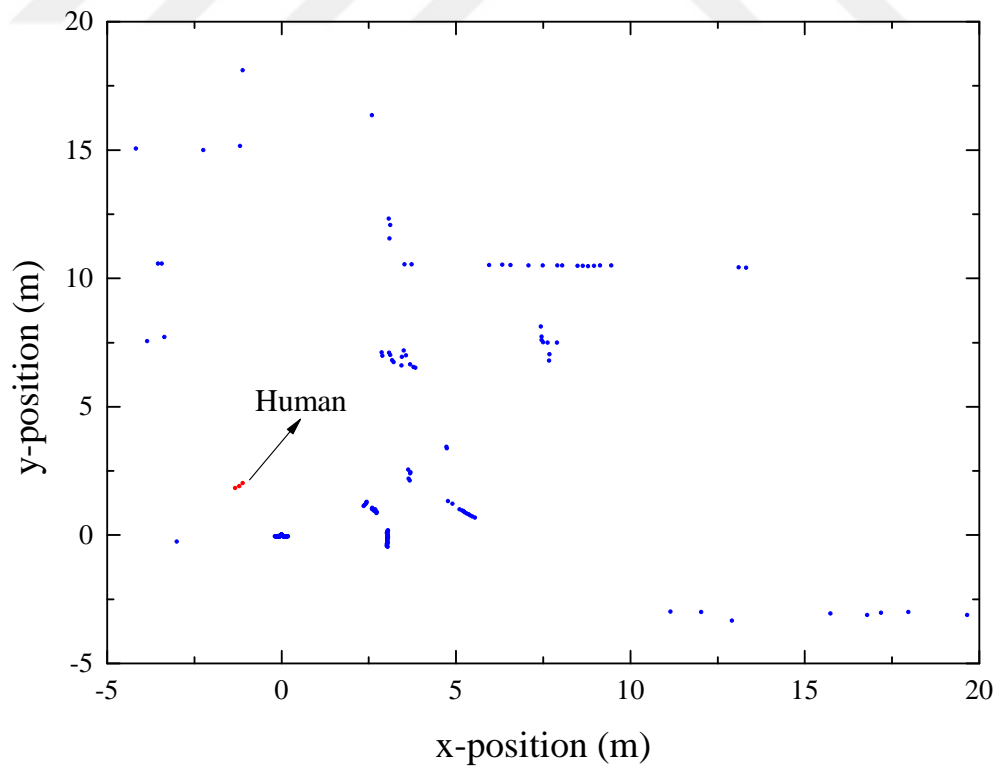


Fig. 3.16.: De-noising Filter, (1634. Frame) - No Noisy Points

The De-noising with Median Filter which is given in Fig. 3.17., has carried some snow noises up in the frame as before, although it eliminates most snow noises. This part is circled in red in the figure. De-noising with LMS Filter, which is shown in Fig. 3.18. has best results still. It removed snowflakes as desired. It is not distort any object in the frame. It also predicted the objects that should behind the snowflakes.

For first artificial snow record, a plotted version of the noise numbers in each frame of filtered and unfiltered data is given in Fig. 3.19. Frames where noise number is zero in all filters are not plotted.

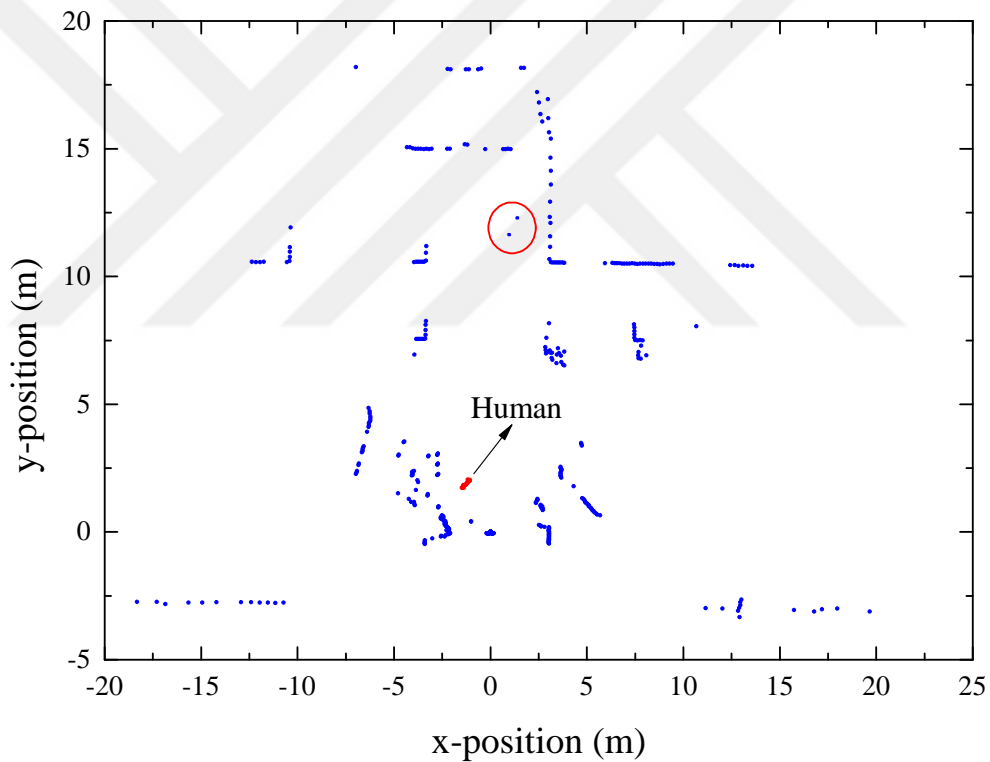


Fig. 3.17.: De-noising with Median Filter, (1634. Frame) - No Noisy Points

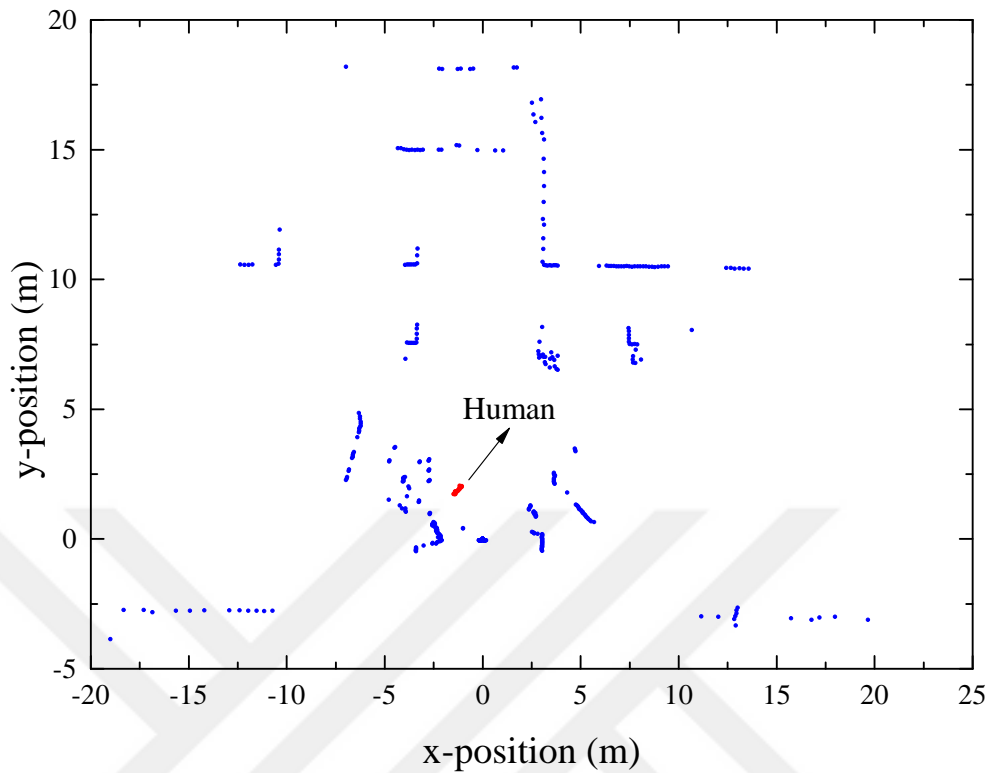


Fig. 3.18.: De-noising with LMS Filter, (1634. Frame) - No Noisy Points

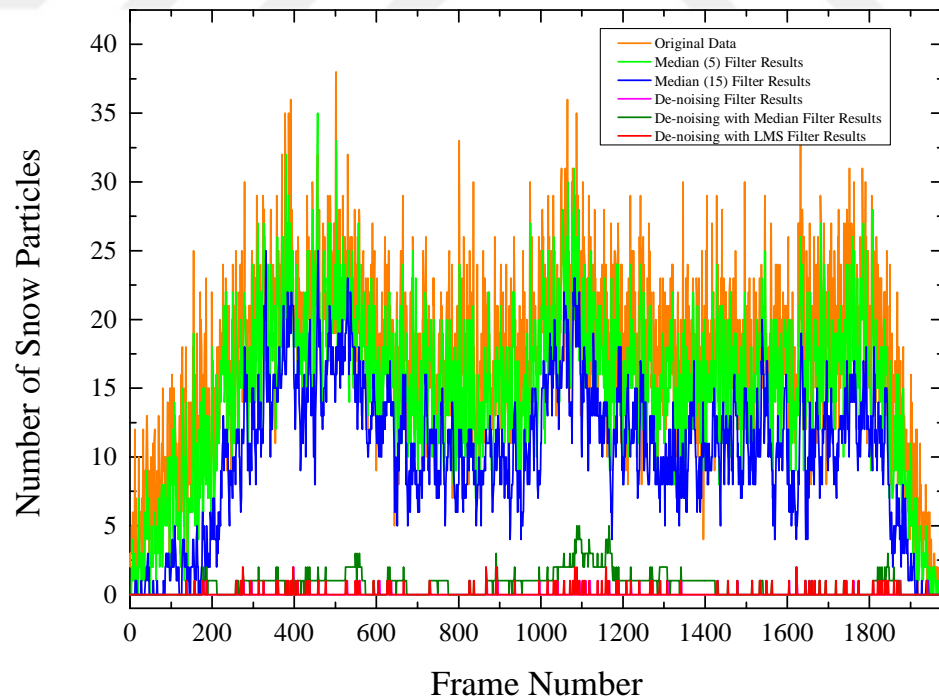


Fig. 3.19.: Noise Numbers of Each Frame at First Artificial Snow Record

According to Artificial Snow - Second Record, with the increase in snowfall, the number of snowflakes per frame increased, the LMS filter showed a better percentage of success than median and caused less delay in time per frame. While LMS filter maintains a success rate of around 98-99%, the success rate of median filter is declining and the time per frame is increasing. The filter size can be increased to improve the results of the median filter, but this will result in more processing load and thus delay. The results of this recording can be viewed from Table 3.3. and the number of noise per frame is shown in Fig. 3.20.

Table 3.3.: Compare of Filters - Artificial Snow 2

	Original Data	De-noising with Median	De-noising with LMS
Total Number of Noisy Points	60137	2250	1039
Snow Density for per Frame	20.694	0.774	0.358
Success Rate (%)	-	96.3	98.3
Total Time (sec)	68.04	138.6	130.7
Time for Each Frame (sec)	0.02	0.041	0.038

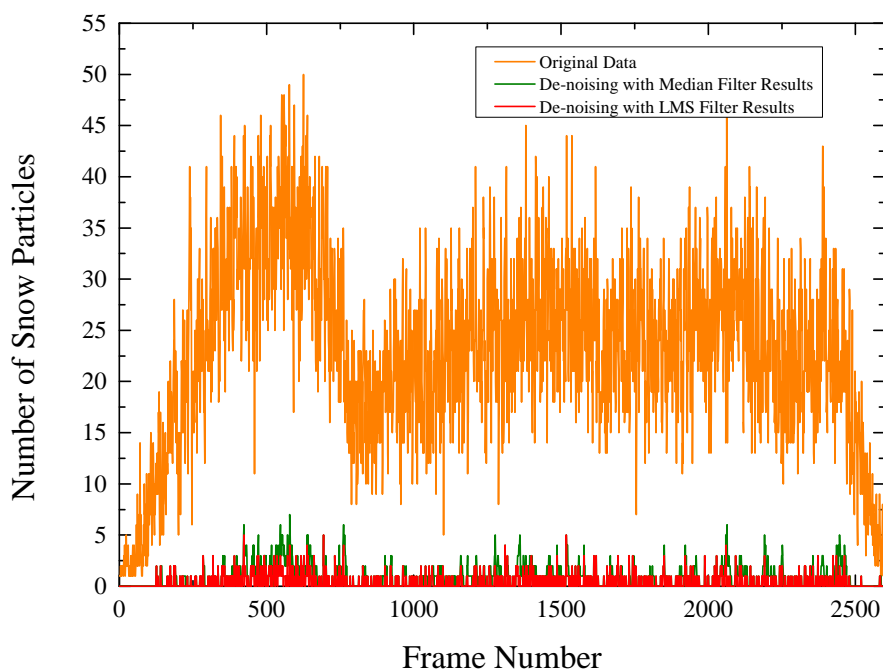


Fig. 3.20.: Noise Numbers of Each Frame at Second Artificial Snow Record

Table 3.4. shows the results of all artificial snow experiments. According to Table 3.4., De-noising with LMS Filter maintains its success rate, no matter how the snow densities and how much snowflakes appear at same point. However, De-noising with Median Filter shows varying success rates depending on the frequency of snow flakes and the intensity of snowfall. The comparison of the two filters according to their success rates and snow density is also shown in Fig. 3.21.

Table 3.4.: Compare of Filters - All Artificial Snow Tests

	Org.	Org.	Med.	LMS	Med.	LMS	Med.	LMS	Med.	LMS
Rec.	Snow Points	Dens.	Noisy Points	Noisy Points	Dens.	Dens.	Time	Time	Succ.	Succ.
1.	34283	17.14	1408	144	0.70	0.07	0.029	0.027	95.89	99.57
2.	60137	20.69	2250	1039	0.78	0.35	0.041	0.038	95.25	98.27
3.	42374	21.19	4141	239	2.07	0.12	0.036	0.032	92.70	99.44
4.	32309	17.66	1810	169	0.99	0.09	0.029	0.026	94.40	99.47
5.	31843	17.18	1747	210	0.94	0.11	0.034	0.031	94.51	99.34
6.	18274	16.84	908	110	0.84	0.10	0.027	0.024	95.03	99.40
7.	17433	19.31	1980	126	2.19	0.14	0.027	0.024	88.64	99.27
8.	25742	20.22	1483	109	1.16	0.09	0.026	0.024	94.24	99.58

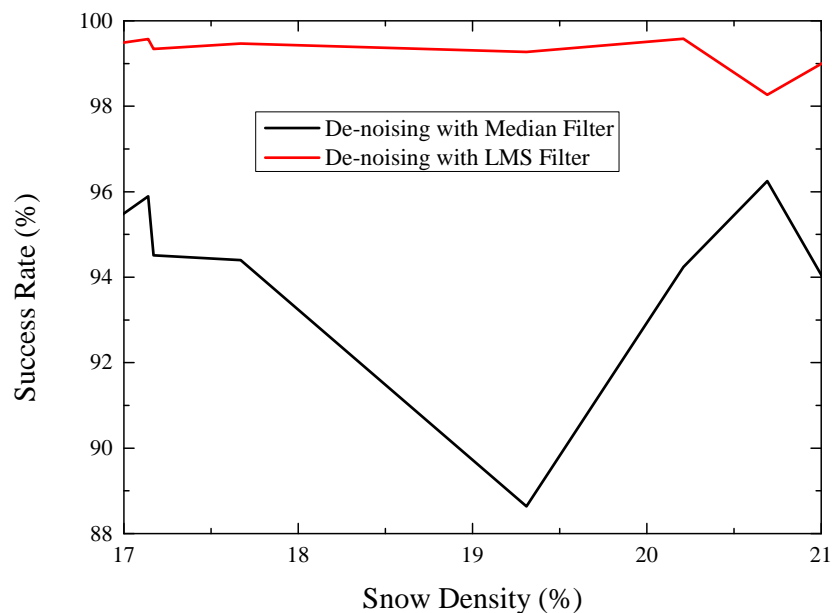


Fig. 3.21.: Comparison of Filter Success Rates due to Snow Density

"Org" is original data. "Med." are De-noising with Median Filter. "LMS" are De-noising with LMS Filter. "Rec" is artificial snow records. "Snow Points" is total

snowflakes at original data. "Dens." are average noises (snowflakes) for each frame. "Noisy Points" are remaining noises after filtering. "Time" are elapsed time (sec) for each frame. "Succ." are success rate (%) of filters.





## IV. CONCLUSION

In order for autonomous vehicles to move safely, it is very important that the sensor data is pure and accurate. Therefore, sensor data in adverse weather conditions is one of the most important and challenging issues for autonomous vehicles. Starting from this, academic studies for LIDAR sensor in snowy weather have been examined and improving these studies has been the main focus of this thesis.

In this study, an algorithm that can remove the snowflakes under any kind of snowfall and predict the objects behind the snowflakes is proposed. Snowflakes are detected by checking with a changing threshold value if it causes sudden changes in distances from the sensor data based on the short history. After it is decided that the snowflakes are noise, the objects behind the snowflakes are tried to be predicted with the help of LMS filter and these objects are replaced with snowflakes. The accuracy of these studies is tested with the LIDAR sensor on the autonomous research vehicle " OKANOM " in the artificial snow environment created. Also the existing median filter results are compared with the proposed method. As a result, The developed De-noising Algorithm improved with Least Mean Squares Filter presents 99% de-noising success even under heavy snowfalls.

### 4.1. Future Work

In future studies, it is planned to improve this algorithm developed for snowy weather further and make it able to detect other adverse weather conditions such as fog, rain, hail and air pollution and eliminate the noise that will occur in the sensor data because of these adverse weather conditions. In order to achieve this goal, it is considered to detect the weather with the help of the camera and to fuse the data from the distance sensors such as LIDAR and radar to achieve the lowest error rate and increase the stability. This study, which is thought to be done, is also planned to test on an autonomous vehicle and

it is aimed to move the vehicle based on the results of this algorithm.



## REFERENCES

- [1] K. Bimbray, "Autonomous cars: Past, present and future - a review of the developments in the last century, the present scenario and the expected future of autonomous vehicle technology," *ICINCO 2015 - 12th International Conference on Informatics in Control, Automation and Robotics, Proceedings*, vol. 1, pp. 191–198, January 2015.
- [2] R. Behringer, "Road recognition from multifocal vision," in *Proceedings of the Intelligent Vehicles '94 Symposium*, October 1994, pp. 302–307.
- [3] W. Zhang, "Sensing for autonomous vehicle navigation," in *2009 Conference on Lasers and Electro-Optics and 2009 Conference on Quantum electronics and Laser Science Conference*, June 2009, pp. 1–2.
- [4] C. Gläser, T. P. Michalke, L. Bürkle, and F. Niewels, "Environment perception for inner-city driver assistance and highly-automated driving," in *2014 IEEE Intelligent Vehicles Symposium Proceedings*, June 2014, pp. 1270–1275.
- [5] P. E. Ross, "Robot, you can drive my car," *IEEE Spectrum*, vol. 51, no. 6, pp. 60–90, June 2014.
- [6] H. Drezet, S. Colombel, and M. Avenel, "Human-man interface concept for autonomous car," in *2019 IEEE International Conference on Consumer Electronics (ICCE)*, January 2019, pp. 1–5.
- [7] J. Funke, P. Theodosis, R. Hindiyeh, G. Stanek, K. Kritatakirana, C. Gerdes, D. Langer, M. Hernandez, B. Müller-Bessler, and B. Huhnke, "Up to the limits: Autonomous audi tts," in *2012 IEEE Intelligent Vehicles Symposium*, June 2012, pp. 541–547.
- [8] G. Tagne, R. Talj, and A. Charara, "Immersion and invariance vs sliding mode

- control for reference trajectory tracking of autonomous vehicles,” in *2014 European Control Conference (ECC)*, June 2014, pp. 2888–2893.
- [9] K. Tomzcak, A. Pelter, C. Gutierrez, T. Stretch, D. Hilf, B. Donadio, N. L. Tenhundfeld, E. J. de Visser, and C. C. Tossell, “Let tesla park your tesla: Driver trust in a semi-automated car,” in *2019 Systems and Information Engineering Design Symposium (SIEDS)*, April 2019, pp. 1–6.
- [10] B. Brown, “The social life of autonomous cars,” *Computer*, vol. 50, no. 2, pp. 92–96, February 2017.
- [11] R. Behringer, S. Sundareswaran, B. Gregory, R. Elsley, B. Addison, W. Guthmiller, R. Daily, and D. Bevely, “The darpa grand challenge - development of an autonomous vehicle,” July 2004, pp. 226 – 231.
- [12] S. L. Poczter and L. M. Jankovic, “The google car: Driving toward a better future?” December 2013, pp. 7–14.
- [13] T. Akgün, Z. Koç, S. Güner, B. Öztürk, B. Ozkan, O. Üstün, N. Tuncay, and U. Özgüner, “A study on autonomous vehicle development process at okan university,” in *2012 IEEE International Conference on Vehicular Electronics and Safety (ICVES 2012)*, July 2012.
- [14] P. Grisleri and I. Fedriga, “The brave autonomous ground vehicle platform,” *IFAC Proceedings Volumes*, vol. 43, no. 16, pp. 497 – 502, 2010, 7th IFAC Symposium on Intelligent Autonomous Vehicles.
- [15] M. Islam, M. Chowdhury, H. Li, and H. Hu, “Cybersecurity attacks in vehicle-to-infrastructure (v2i) applications and their prevention,” *Transportation Research Record: Journal of the Transportation Research Board*, November 2017.
- [16] L. Mearian. (02/29/16, accessed on 07/05/19) Google’s self-driving car has caused its first accident. [Online]. Available: <https://www.computerworld.com/>

article/3039236/googles-self-driving-car-has-caused-its-first-accident.html

- [17] J. Brown. (07/01/16, accessed on 07/05/19) Tesla driver dies in first fatal crash while using autopilot mode. [Online]. Available: <https://www.theguardian.com/technology/2016/jun/30/tesla-autopilot-death-self-driving-car-elon-musk>
- [18] D. Wakabayashi. (03/19/18, accessed on 07/05/19) Self-driving uber car kills pedestrian in arizona, where robots roam. [Online]. Available: <https://www.nytimes.com/2018/03/19/technology/uber-driverless-fatality.html>
- [19] S. Zang, M. Ding, D. Smith, P. Tyler, T. Rakotoarivelo, and M. A. Kaafar, "The impact of adverse weather conditions on autonomous vehicles: How rain, snow, fog, and hail affect the performance of a self-driving car," *IEEE Vehicular Technology Magazine*, vol. 14, no. 2, pp. 103–111, June 2019.
- [20] C. Dannheim, C. Icking, M. Mäder, and P. Sallis, "Weather detection in vehicles by means of camera and lidar systems," in *2014 Sixth International Conference on Computational Intelligence, Communication Systems and Networks*, May 2014.
- [21] R. H. Rasshofer, M. Spies, and H. Spies, "Influences of weather phenomena on automotive laser radar systems," *Advances in Radio Science*, vol. 9, July 2011.
- [22] M. Kutila, P. Pyykönen, W. Ritter, O. Sawade, and B. Schäufele, "Automotive lidar sensor development scenarios for harsh weather conditions," in *2016 IEEE 19th International Conference on Intelligent Transportation Systems (ITSC)*, November 2016.
- [23] B. Yamauchi, "All-weather perception for man-portable robots using ultra-wideband radar," in *2010 IEEE International Conference on Robotics and Automation*, May 2010.
- [24] S. Ronnback and A. Wernersson, "On filtering of laser range data in snowfall," in *2008 4th International IEEE Conference Intelligent Systems*, September 2008.

- [25] S. Michaud, J.-F. Lalonde, and P. Giguère, “Towards characterizing the behavior of lidars in snowy conditions,” in *IEEE-RSJ-IROS Workshop on Planning, Perception and Navigation for Intelligent Vehicles*, September 2015.
- [26] M. Aldibaja, N. Suganuma, and K. Yoneda, “Improving localization accuracy for autonomous driving in snow-rain environments,” in *2016 IEEE/SICE International Symposium on System Integration (SII)*, December 2016.
- [27] M. Aldibaja, N. Suganuma, and K. Yoneda, “Robust intensity-based localization method for autonomous driving on snow-wet road surface,” *IEEE Transactions on Industrial Informatics*, vol. PP, June 2017.
- [28] N. Charron, S. Phillips, and S. L. Waslander, “De-noising of lidar point clouds corrupted by snowfall,” in *2018 15th Conference on Computer and Robot Vision (CRV)*, May 2018.
- [29] L. Hespel, N. Riviere, T. Huet, B. Tanguy, and R. Ceolato, “Performance evaluation of laser scanners through the atmosphere with adverse condition,” *Proc SPIE*, vol. 8186, October 2011.
- [30] F. Fayad and V. Cherfaoui, “Tracking objects using a laser scanner in driving situation based on modeling target shape,” in *2007 IEEE Intelligent Vehicles Symposium*, June 2007.
- [31] T. Sjöstedt, “Lidar signal processing techniques : Clutter suppression, clustering and tracking,” p. 76, 2011.
- [32] P. Sudhakar, K. A. Sheela, and M. Satyanarayana, “Imaging lidar system for night vision and surveillance applications,” in *2017 4th International Conference on Advanced Computing and Communication Systems (ICACCS)*, January 2017.
- [33] J. Bossu, N. Hautière, and J.-P. Tarel, “Rain or snow detection in image sequences through use of a histogram of orientation of streaks,” *International Journal of*

*Computer Vision*, vol. 93, pp. 348–367, July 2011.

- [34] M. Langer and L. Zhang, “Rendering falling snow using an inverse fourier transform,” June 2003.
- [35] M. Langer, L. Zhang, A. W. Klein, A. Bhatia, J. Pereira, and D. Rekhi, “A spectral-particle hybrid method for rendering falling snow.” January 2004, pp. 217–226.
- [36] N. Wang and B. Wade, “Rendering falling rain and snow,” p. 14, August 2004.
- [37] C. Wang, Z. Wang, T. Xia, and Q. Peng, “Real-time snowing simulation,” *The Visual Computer*, vol. 22, no. 5, pp. 315–323, May 2006.
- [38] H. Hase, K. Miyake, and M. Yoneda, “Real-time snowfall noise elimination,” in *Proceedings 1999 International Conference on Image Processing (Cat. 99CH36348)*, vol. 2, October 1999.
- [39] L. Xudong, Z. Xuedong, and W. Youchuan, “A kind of filtering algorithms for lidar intensity image based on flatness terrain,” January 2005.
- [40] X. Lai and M. Zheng, “A denoising method for lidar full-waveform data,” *Mathematical Problems in Engineering*, vol. 2015, pp. 1–8, July 2015.
- [41] M. F. Dionizio, A. Shamsoddini, and J. C. Trinder, “Noise reduction algorithm for full-waveform lidar signal,” in *2011 IEEE International Conference on Signal and Image Processing Applications (ICSIPA)*, November 2011.
- [42] X. Ma, C. Xiang, and W. Gong, “A universal de-noising algorithm for ground-based lidar signal,” *ISPRS - International Archives of the Photogrammetry, Remote Sensing and Spatial Information Sciences*, vol. XLI-B1, pp. 53–56, June 2016.
- [43] N. Gallagher and G. Wise, “A theoretical analysis of the properties of median filters,” *IEEE Transactions on Acoustics, Speech, and Signal Processing*, vol. 29,

- no. 6, pp. 1136–1141, December 1981.
- [44] T. Nodes and N. Gallagher, “Median filters: Some modifications and their properties,” *IEEE Transactions on Acoustics, Speech, and Signal Processing*, vol. 30, no. 5, pp. 739–746, October 1982.
- [45] M. Stork, “Median filters theory and applications,” January 2003.
- [46] R. Rahim and A. Ikhwan, “Implementation of modified median filtering algorithm for salt & pepper noise reduction on image,” September 2017.
- [47] R. Rahmat, A. Malik, and N. Kamel, “Comparison of lulu and median filter for image denoising,” *International Journal of Computer and Electrical Engineering*, pp. 568–571, January 2013.
- [48] G. Gupta, “Algorithm for image processing using improved median filter and comparison of mean, median and improved median filter,” 2011.
- [49] J. Astola, P. Haavisto, and Y. Neuvo, “Vector median filters,” *Proceedings of the IEEE*, vol. 78, no. 4, pp. 678–689, April 1990.
- [50] Y. Liu, “Noise reduction by vector median filtering,” *GEOPHYSICS*, vol. 78, no. 3, pp. V79–V87, 2013.
- [51] S. Haykin, *Adaptive filter theory*, 4th ed. Upper Saddle River, NJ: Prentice Hall, 2002.
- [52] P. S. R. Diniz, *Adaptive Filtering*, 4th ed. Springer US, 2013, ch. 3-4, pp. 79–207.
- [53] S. Haykin and B. Widrow, *Least-Mean-Square Adaptive Filters*. John Wiley & Sons, Inc., 2003.
- [54] S. Dixit and D. Nagaria, “Lms adaptive filters for noise cancellation: A review,” *International Journal of Electrical and Computer Engineering (IJECE)*, vol. 7, p. 2520, October 2017.



- [55] A. Nealen, “An as-short-as-possible introduction to the least squares, weighted least squares and moving least squares methods for scattered data approximation and interpolation,” January 2004.
- [56] Y. Li, J. Li, L. Wang, J. Zhang, D. Li, and M. Zhang, “A weighted least squares algorithm for time-of-flight depth image denoising,” *Optik*, vol. 125, no. 13, pp. 3283 – 3286, 2014.
- [57] P. Sallis, C. Dannheim, C. Icking, and M. Maeder, “Air pollution and fog detection through vehicular sensors,” in *2014 8th Asia Modelling Symposium*, September 2014, pp. 181–186.
- [58] SICK. (accessed on July, 2019) Operating instructions, lms1xx laser measurement sensors. [Online]. Available: [https://cdn.sick.com/media/docs/1/31/331/Operating\\_instructions\\_LMS1xx\\_Laser\\_Measurement\\_Sensors\\_en\\_IM0031331.PDF](https://cdn.sick.com/media/docs/1/31/331/Operating_instructions_LMS1xx_Laser_Measurement_Sensors_en_IM0031331.PDF)
- [59] sick. (accessed on July, 2019) 2d lidar sensors, lms1xx / outdoor. [Online]. Available: <https://www.sick.com/cz/en/detection-and-ranging-solutions/2d-lidar-sensors/lms1xx/lms111-10100/p/p109842>
- [60] Sick. (accessed on July, 2019) Lms1xx, compact and economical, even in harsh environments. [Online]. Available: [https://cdn.sick.com/media/docs/5/15/415/Product\\_information\\_LMS1xx\\_2D\\_laser\\_scanners\\_en\\_IM0026415.PDF](https://cdn.sick.com/media/docs/5/15/415/Product_information_LMS1xx_2D_laser_scanners_en_IM0026415.PDF)
- [61] Nvidia. (accessed on July, 2019) Jetson tx1 gelistirici kiti. [Online]. Available: <https://www.nvidia.com.tr/object/jetson-tx1-dev-kit-tr.html>
- [62] O. S. R. Foundation and A. Dattalo. (August, 2018 - accessed on July, 2019) Ros - introduction. [Online]. Available: <http://wiki.ros.org/ROS/Introduction>
- [63] O. S. R. Foundation and J. Sprickerhof. (June, 2015 - accessed on July, 2019) Rosbag. [Online]. Available: <http://wiki.ros.org/rosbag>

- [64] O. S. R. Foundation and M. Purvis. (May, 2015, accessed on July, 2019) Lms1xx. [Online]. Available: <http://wiki.ros.org/LMS1xx>
- [65] G. Yadav and B. Ananda Krishna, “Study of different adaptive filter algorithms for noise cancellation in real-time environment,” *International Journal of Computer Applications*, vol. 96, January 2014.
- [66] B. Atila, T. E. Mungan, and O. C. K1vanç, “Different filter approaches and performance analysis of fundamental sensors in autonomous ground vehicles,” in *2016 24th Signal Processing and Communication Application Conference (SIU)*, May 2016, pp. 1605–1608.

## VITA

Cemre Kavvasođlu received his Bachelor of Science degree in Mechatronics Engineering from Istanbul Okan University, Istanbul, Turkey, in June 2017. He worked in the Power Electronics and Electromechanical Energy Conversion (PEEC) Laboratory, in the Department of Mechatronics Engineering at Istanbul Okan University, with Asst. Prof. Dr. Ömer Cihan Kıvanç as his advisor. He is currently working at Istanbul Okan University as a research assistant since 2017.

Cemre Kavvasođlu is a student member of the IEEE.

